of derivatization prevents salt formation, which complicates the mass spectrum and impairs the signal-to-noise ratio for the individual molecular ion species. Furthermore, the lack of hydroxyl groups also prevents the cleavage of other glycosidic bonds (Lemoine et al. 1996), making the permethylated oligosaccharides resistant to in-source fragmentation. In fact, the sialylation levels determined by MALDI MS after permethylation were acceptable, although a variance exists among laboratories, as was the case for chromatography. A special setup of derivatization required a smaller amount of samples (5 μg glycoprotein) to meet the high sensitivity of MALDI MS for permethylated oligosaccharides (Kang et al. 2005), whereas routine analysis used approximately 100 μg in this study.

The levels of triantennary oligosaccharides determined by MALDI MS were lower than those from chromatography, though not markedly. It is not possible to decide which value is the correct one, but the decreased triantennary structures seen by MS may be due to the increased mass of 810.4 Da of an additional antenna, making the detector response for the triantennary oligosaccharide ions at m/z 3602.8 weaker than that for the biantennary ions at m/z 2792.4, or there may be increased collision-induced dissociation (CID) of an enlarged cross-section of structure. The peak broadening effect due to isotopes is only 17% for this mass increase and thus does not produce a substantial error even when the quantitation is based on the peak height in the MALDI mass spectrum. On the other hand, core fucosylation, which occurs at the sixth position of the reducing terminal GlcNAc in the transferrin oligosaccharides, does not affect quantitation by MALDI MS (Naven and Harvey 1996). It is worth noticing that the level of the triantennary oligosaccharide was lower than that of the fucosylated species in measurements with either MALDI MS or chromatography, indicating that MALDI MS is similar in its ability to detect minor glycans. Similarly, good relative quantitation by MALDI MS was confirmed by IgG analysis, as the monogalactosylated species was the most abundant and the calculated level of galactosylation was comparable to that obtained by chromatography.

ESI MS was employed by two laboratories, where oligosaccharide alditols were separated by graphitized carbon chromatography and introduced on-line to an ESI mass spectrometer operated in the negative ion mode (Karlsson et al. 2004). The reproducibility of LC/ESI MS was acceptable from the data of lab 16. Regarding sialylated oligosaccharides, ESI is soft enough to detect the intact oligosaccharides with sialylation unless high nozzle-skimmer potential is applied, even when sialic acids are not derivatized. However, the charge of sialic acids affects the efficiency of negative ion formation, and thus the distribution of multiple-charge ions in the mass spectrum is different from that for neutral oligosaccharides, disturbing straightforward quantitation of sialic acid-substituted oligosaccharides in the mass spectrum or ion chromatogram at the same time as neutral glycans. Nevertheless, LC/ESI MS results were comparable to those from MALDI MS or chromatography as shown in Figures 1B and 2B, except that an increased level of monosialylated oligosaccharides from the transferrin sample was reported by one laboratory, possibly due to sialic acid loss during sample preparation. A brief summary of the methods for oligosaccharide analysis including capillary electrophoresis-MS (Zamfir et al. 2000) is presented in Table V.

In this study, some laboratories also presented MS/MS spectra of permethylated or reductively aminated oligosaccharides. For example, the product ion mass spectra provided branching and linkage information (Supplementary Figure 4). This method is used for structure verification, qualitatively, and is not primarily directed toward quantitation. However, along with the establishment of the strategies for *de novo* carbohydrate sequencing by an algorithm incorporating the fragmentation database and informatics (Ashline et al. 2005; Tang et al. 2005), quantitation of oligosaccharide isomers will be realized in the near future.

Glycopeptides

Glycopeptide analysis allows the identification of site-specific oligosaccharide structures, which are essential to understand the role of local oligosaccharide structures in protein folding and functions. However, it is conceivable that the analysis of glycopeptides is difficult as compared to that of unglycosylated peptides or oligosaccharides, since chemical properties differ between the glycan and peptide components. Moreover, each glycopeptide is often a minor constituent in the peptide mixtures after enzymatic digestion of glycoproteins because of the large number of glycoforms expressed by many proteins at each site. These problems may be overcome by employing LC/MS and selecting the glycopeptides in the chromatogram by detection of the CID-generated glycan-specific oxonium ions (Huddleston et al. 1993). Alternatively, glycopeptide fraction can be enriched by lectin or other extraction tools, and the fraction can be directly analyzed by MS, especially when the glycoprotein has a small number of glycosylation sites, as is the case for transferrin and IgG (Wada et al. 2004). The glycan and peptide structures of glycoproteins can then be elucidated by MS/MS of glycopeptide ions (Liu et al. 1993; Krokhin et al. 2004).

MS of glycopeptides is usually performed in the positive ion mode to detect $[M+H]^+$ ions. In this case, protonation occurs on the peptide portion, and thus the signal intensity of the glycopeptide is largely dependent on the proton affinity of the peptide component of the molecule, thus rationalizing the quantitation of different glycoforms of a peptide according to their signal intensities. However, there are still a few concerns. First, glycopeptides are larger than oligosaccharides and thus are accompanied by an increased risk of CID. Since the glycan moiety is more labile than the peptide backbone, the resulting cleavage of the glycosidic bonds may result in overestimation of the glycoforms with a smaller number of building saccharides. This effect will be evident in the MALDI produced ions, in which internal energies are higher than those of ESI ions. In previous reports, however, neutral oligosaccharides had minimal affect upon the ionization efficiencies of glycopeptides, and consequently, the integration of MALDI TOF signals of several desialylated glycopeptides yielded excellent quantitative correlations with published data obtained by established high-performance liquid chromatography (HPLC) techniques (Sutton et al. 1994; Harmon et al. 1996). Second, the sialic acids of glycopeptides cannot be appropriately derivatized without deleterious modifications of the peptide component. In MALDI MS, the sialic acid loss occurs both in-source and postsource as described above, and occurs over a significant time frame in which a hydrogen transfers between suitably positioned functional groups (Harvey

Table V. Methods for structural analysis and quantitation of oligosaccharides

	Advantages	Disadvantages
Reductive amination and fluorescence-labeling/chromatography	Standard method for quantitation (if appropriately prepared); possible isomer discrimination; Independence of detector response on glycan size or structure	Various conditions for derivatization
Permethylation / +MALDI-TOF MS	Invariant conditions for derivatization available; protection of weak glycosidic linkages (e.g. sialic acid)	Loss of alkali-labile substituents
		Discrimination of isobaric species unable without MS/MS; instruments available
		Inverse correlation of detector response to molecular mass
No derivatization/ + MALDI-TOF MS	Easy and quick	Less sensitive
		Glycosidic bond cleavage, if not the matrix choice approapriate
Reducing end derivatization / +MALDI-TOF MS	Possible sharing of samples with chromatography when fluorescence-labeled	Glycosidic bond cleavage, if not the matrix choice appropriate
Direct inlet nanoESI MS and MS/MS	No loss of sample due to derivatization; detailed sequence analysis; superior sensitivity by sprayer chips	
No derivatization/LC/-ESI MS(/MS)	Easy MS/MS acquisition for structure elucidation; data-dependent analysis after run	Different charge distribution between neutral and acidic glycans; requirement of nanospray for good sensitivity
CE-MS and MS/MS	No loss of sample due to derivatization; detailed sequence analysis; high flexibility of protocols	

1999). Consequently, the sialic acid loss increases with the longer delay time before extraction (Naven et al. 1997); and is prominent in the MALDI ion-trap type of mass separators. Most studies of sialylated glycopeptides with MALDI TOF MS are conducted in the linear mode so that the postsource decay ions are not separated. On the other hand, the sialic acid loss is minimal in ESI, but there are charge-dependent effects on the ionization efficiency and on the distribution of multiple-charge ions of the oligosaccharides.

Despite these problems, the site-specific analysis of glycoprotein oligosaccharides by MS is becoming popular. In the present study, the results from two laboratories on glycopeptides, one with MALDI MS and another with LC/MS, were consistent with each other, and were informative in terms of the oligosaccharide profiles specific to the protein sequence. The galactosylation levels at different polymorphic sequences of IgG explained well the global glycan profiles determined by the analyses of released oligosaccharides, and the oligosaccharide profiles of two glycosylation sites of transferrin were clearly shown to be different from each other. Although these findings could be obtained by isolation of each glycopeptide and subsequent analysis of released oligosaccharides, the direct analysis of glycopeptides performed herein is by far easier and more rapid as well as being sufficiently sensitive for minor glycans. The glycopeptide analysis requires a fairly small amount of samples (less than 10 μg glycoprotein in this study), and thus will contribute a great deal to the emerging field of glycoproteomics.

In conclusion, MALDI MS of permethylated oligosaccharides is as reliable as chromatographic methods for elucidating glycan profiles based on mass mapping of the compositional analysis. The publicly available murine and human MALDI MS glycomics data, which is being acquired by the Consortium for Functional Glycomics (www.functionalglycomics.org), for systems biology research are based on this approach. Good relative quantitation data can be achieved without neutralization of sialic acid residues by LC/ESI MS utilizing porous graphitized carbon as a separation medium for oligosaccharide alditols. Quantitative and relative quantitative datasets can be obtained by peptide sequencing and determination of glycosylation sites by LC-MS/MS of native glycopeptides. Analysis of glycopeptides is not yet widely implemented outside specialist glycobiology laboratories, but it is clear from both the present study and the increasing volume of publication in this area that glycoproteomic strategies are now sufficiently mature to allow practical site-specific characterization of the oligosaccharide profiles of even highly heterogeneous glycoproteins (Harazono et al. 2005; Imre et al. 2005; Tajiri et al. 2005; Chalabi et al. 2006). Our present results justify the use of MS for relative quantitation of oligosaccharides, and highlight that glycopeptide MS will be a key interfacing technique in proteomics and functional glycomics in the future.

Methods

Glycoprotein samples

The blood samples were obtained from three healthy Japanese donors (A, B, and C) with the permission from the Medical Ethics Committee of Osaka University Graduate School of Medicine. Transferrin and IgG were purified from individual serum by immunoaffinity with rabbit polyclonal antibody against human transferrin and by protein G affinity chromatography, respectively, and then lyophilized. The purity of distributed samples was validated by sodium dodecyl sulfate–polyacrylamide gel electrophoresis (SDS–PAGE) under reducing conditions. Each 1 mg sample from six specimens (A, B, and C for transferrin and IgG) in total was delivered to 26 laboratories at ambient temperature. Twenty of these laboratories

submitted results. The stability of these materials during transport was guaranteed by a test incubation, during which neither degradation nor modification of protein and glycan moieties was observed after one week of storage at 37 °C. In most laboratories, a 100 μg sample was used for each analysis.

Release of oligosaccharides

A majority of laboratories employed the method of oligosaccharide release from enzymatic digests of glycoproteins, typically as follows. Proteins (0.5 mg of transferrin or IgG) were dissolved in 0.5 mL of 6 M guanidium hydrochloride, 0.25 M Tris–HCl, pH 8.5 and reduced with 5 mg of dithiothreitol under N_2 at room temperature for 3 h. Then, 9 mg of iodoacetamide were added to the solution, followed by incubation in the dark at room temperature for 30 min for carbamidomethylation. The reagents were removed by a gel fitration column, NAP-5 (GE Healthcare, Piscataway, NJ), equilibrated with 0.05 N HCl, and the recovered proteins were lyophilized. The alkylated proteins were dissolved in 50 mM ammonium hydrogen carbonate, pH 8.0, and digested with 10 μg of trypsin at 37°C for 3 h. Subsequently, 20 U of Peptide: *N*-Glycosidase F (PNGase F) (*N*-glycanase F) (Roche, Mannheim, Germany) were added to the solution, followed by incubation at 37°C for 12 h to release *N*-linked oligosaccharides from glycopeptides. The solution was then passed through a solid phase extraction Sep-Pak Light C18 cartridge (Waters, Millford, MA), and the oligosaccharides in the pass-through fraction were recovered and lyophilized.

When oligosaccharides were released directly from glycoproteins, the in-solution or in-gel release method was used. For in-solution release, the 0.5 mg protein samples were dissolved in 400 μL of water and 40 μL of 10× denaturing solution (5% SDS and 10% β-mercaptoethanol). The sample was then denatured at 100°C for 5 min. After cooling, a 40 μL of reaction buffer (0.5 M sodium phosphate, pH 7.5) containing 10% Nonidet P-40 were added. The sample was mixed and incubated with PNGase F at 37 °C for 12 h. The digested sample solution was run through a C18 cartridge to remove the detergent, and then lyophilized (Sheeley and Reinhold 1998). The sample was desalted on a graphitized carbon column or by the normal phase extraction method (Wada et al. 2004).

For in-gel release (Royle et al. 2006), 80 μg samples were reduced with 0.5 M dithiothreitol for 10 min at 70 °C, alkylated with 100 mM iodacetamide for 30 min at room temperature, then run over three lanes on 10% SDS–PAGE gels and visualized with Coomassie blue. Protein bands were excised, cut into approximately 1 mm^3, frozen for 2 h at −20 °C, then washed with alternating 1 mL acetonitrile and 1 mL 20 mM $NaHCO_3$ pH 7 (five washes, 30 min each) and the gel pieces lyophilized. *N*-linked glycans were released *in situ* with 100 U/mL PNGase F with overnight incubation. Glycans were extracted by washing with 3× 0.2 mL water, 1× 0.2 mL acetonitrile, 1× 0.2 mL water, 1× 0.2 mL acetonitrile (30 min each). Samples were lyophilized ready for MS or fluorescent labeling.

Fluorescence labeling and chromatography of oligosaccharides

For fluorescence detection, the oligosaccharides were subjected to reductive amination at the reducing end with 2-aminopyridine (Natsuka and Hase 1998), 2-aminobenzamide (Bigge et al. 1995) or 2-aminobenzoate (Anumula and Dhume 1998). The typical procedure using 2-aminobenzoate are as follows. To the lyophilized oligosaccharides, a solution (200 μL) of 2-aminobenzoate and sodium cyanoborohydride, freshly prepared by dissolution of both reagents (30 mg each) in methanol (1 mL) containing sodium acetate and 2% boric acid was added. The mixture was kept at 80 °C for 1 h. After cooling, the solution was applied to a column of Sephadex LH-20 (1 × 30 cm) equilibrated with 50% methanol. Earlier eluted fractions showing fluorescence at 410 nm with 335 nm-wavelength irradiation were collected and evaporated to dryness. The residue was dissolved in water (100 μL), and a portion (10 μL) was analyzed by HPLC. Separation was done at 50°C with a polymer-based Asahi Shodex NH2P-50 4E column (Showa Denko, Tokyo; 4.6 × 250 mm) using a linear gradient formed by 2% acetic acid in acetonitrile (solvent A) and 5% acetic acid in water containing 3% triethylamine (solvent B). The column was initially equilibrated and eluted with 70% solvent A for 2 min, at which point solvent B was increased to 95% over 80 min and kept at this composition for a further 100 min. The flow rate was 1.0 mL/min throughout the analysis. Detection was performed by fluorometry with $\lambda_{ex} = 350$ nm and $\lambda_{em} = 425$ nm.

The oligosaccharides derivatized with 2-aminopyridine were analyzed by multidimensional chromatography (Takahashi 1996). In some laboratories, the separated oligosaccharide were analyzed by MALDI TOF MS for structure verification.

MALDI MS of permethylated oligosaccharides

Permethylation was performed by the solid sodium hydroxide technique (Dell et al. 1993; Lemoine et al. 1996; Ciucanu and Costello 2003). Briefly, five pellets (approximately 1 g) of NaOH were ground in a dry mortar to obtain a fine powder. This should be done as quickly as possible to minimize absorption of moisture from the atmosphere. The NaOH powder was mixed with 4 mL of anhydrous dimethyl sulfoxide. The oligosaccharide sample released from glycoproteins was dried in a glass tube. Approximately 1 mL of the slurry was added to the sample followed by 0.5 mL of iodomethane. The sample was agitated at room temperature for 10 min. The reaction was then terminated by addition of 2 reaction volumes of water. Subsequently, 1 mL of chloroform was added, and the mixture was vortexed for 30 s and centrifuged at 3000*g* to facilitate partitioning. The top aqueous layer was removed and the chloroform layer was then washed three additional times with 4 mL of water. The chloroform was evaporated to obtain a dried permethylated sample. One laboratory used the capillary permethylation method as described previously (Kang et al. 2005).

For MALDI MS, the dried permethylated sample was resuspended in 10 μL of pure methanol. The sample was mixed with an equal volume of DHB matrix solution at 20 mg/mL in 80% methanol and then spotted onto the MALDI plate. To attain good ion statistics the spectra presented were generated from several sub-spectra of 100 laser shots. The peak height of the $[M+Na]^+$ monoisotopic ions or the integrated peak area for their entire isotopic cluster was measured for relative quantitation.

Reproducibility of the quantitation was examined in one laboratory (lab 17) as follows. Sample B IgG (0.3 mg) was divided into three portions, and each sample was separately subjected to permethylation according to the procedures described above. The MALDI spectrum was acquired with a Voyager DE Pro mass spectrometer (Applied Biosystems, Foster City, CA) in reflectron mode. The signals from a total of 500 shots at 10 different laser irradiation spots were averaged, and the measurement was repeated five times.

The oligosaccharides derivatized at the reducing end or those with intact nonreducing hydroxyls were analyzed by MALDI MS in a few laboratories, among which a simple on-target derivatization with phenylhydrazine was carried out in lab 10 (Lattová et al. 2006).

Analysis of oligosaccharides by LC/ESI MS or LC/ESI MS/MS

The alditol forms of oligosaccharides were analyzed by LC/ESI MS (Karlsson et al. 2004). Typically, the enzymatically released oligosaccharides were converted into alditols by incubation in 20 μL of 0.5 M sodium borohydride/20 mM potassium hydroxide solution at 50 °C for 2 h. The resulting solutions were neutralized by addition of 1 mL of glacial acetic acid, desalted and dried. Borate was removed by repeated addition and evaporation of 50 μL of 1% acetic acid in methanol. Oligosaccharide samples were dissolved in water and subjected to negative ion LC/MS employing a graphitized carbon column (Hypercarb, Thermo Electron; 0.2 × 150 mm), using a linear gradient formed by 5 mM ammonium acetate/2% acetonitrile (solvent A) and 5 mM ammonium acetate/80% acetonitrile (solvent B) (Kawasaki et al. 1999). The deprotonated $[M-H]^-$ ions were measured, and the peak areas of the multiple-charge ions corresponding to one specific component were summed up manually for relative quantitation data.

MS of glycopeptides

Glycoproteins were reduced and alkylated, and then digested with trypsin as described above. Resulting peptide/glycopeptide mixtures were analyzed with LC/MS(/MS) or MALDI MS (Huddleston et al. 1993; Wada et al. 2004; Harazono et al. 2005). In either case, protonated peptides were monitored for detection. In LC/MS, glycopeptide profiles can be inferred from a low CID energy MS survey, while the molecular weight contribution of the core peptide can usually be inferred from the MS/MS data. Relative quantitation was carried out in the same way as LC/MS of oligosaccharides. For MALDI MS, glycopeptides were enriched from an enzymatic digest and the resulting glycopeptide mixture was mixed with DHB matrix solution at 10 mg/mL in 0.1% trifluoroacetic acid/50% acetonitrile and analyzed in linear mode (Wada et al. 2004). Relative quantitation was based on the intensities (heights) of the signals.

Data presentation

The relative abundances of the glycoforms identified were reported by each participating laboratory.

Acknowledgments

The authors thank Trina Abney, David Ashline, Shiu-Yun Chan, John F. Cipollo, Naoko Goto-Inoue, David J. Harvey, Soo Kyung Hwang, Satsuki Itoh, Pilsoo Kang, Mitsuhiro Kinoshita, Hui-Chung Liang, Chia-Wei Lin, Miyako Nakano, Osamu Nishimura, Maria Panico, Louise Royle, Radka Saldova, Mark Sutton-Smith, Minoru Suzuki, Yusuke Suzuki, Michiko Tajiri, Noriko Takahashi, Berangere Tissot, Hirokazu Yagi, and Bo Xie for their help in carrying out the experimental work and for discussion. A part of this work was supported by the 21st century COE Program of Osaka University from the Japan Society for the Promotion of Science (JSPS) and by the JSPS Core-to-Core program.

Supplementary data

Supplementary data are available at Glycobiology online (http://glycob.oxfordjournals.org).

Conflict of interest statement

None declared.

Abbreviations

CID, Collision-induced dissociation; DHB, 2,5-dihydroxybenzoic acid; LC, liquid chromatography; Fab, fragment antigen binding; Fc, fragment crystallizable; HPLC, high-performance liquid chromatography; ESI, electrospray ionization; HGPI, Human Disease Glycomics/Proteome Initiative; HUPO, Human Proteome Organisation; IgG, immunoglobulin-G; MALDI, matrix-assisted laser desorption/ionization; MS, mass spectrometry; PNGase F, Peptide: *N*-Glycosidase F; SD, standard deviation; SDS–PAGE, sodium dodecyl sulfate–polyacrylamide gel electrophoresis; TOF, time-of-flight.

References

Anumula KR, Dhume ST. 1998. High resolution and high sensitivity methods for oligosaccharide mapping and characterization by normal phase high performance liquid chromatography following derivatization with highly fluorescent anthranilic acid. Glycobiology. 8:685–694.

Apweiler R, Hermjakob H, Sharon N. 1999. On the frequency of protein glycosylation, as deduced from analysis of the SWISS-PROT database. Biochim Biophys Acta. 1473:4–8.

Ashline D, Singh S, Hanneman A, Reinhold V. 2005. Congruent strategies for carbohydrate sequencing. 1. Mining structural details by MS(n). Anal Chem. 77:6250–6262.

Axford JS. 1999. Glycosylation and rheumatic disease. Biochim Biophys Acta. 1455:219–229.

Bigge JC, Patel TP, Bruce JA, Goulding PN, Charles SM, Parekh RB. 1995. Nonselective and efficient fluorescent labeling of glycans using 2-amino benzamide and anthranilic acid. Anal Biochem. 230:229–238.

Brooks SA. 2004. Appropriate glycosylation of recombinant proteins for human use: implications of choice of expression system. Mol Biotechnol. 28:241–255.

Chalabi S, Panico M, Sutton-Smith M, Haslam SM, Patankar MS, Lattanzio FA, Morris HR, Clark GF, Dell A. 2006. Differential *O*-Glycosylation of a conserved domain expressed in murine and human ZP3. Biochemistry. 45:637–647.

Ciucanu I, Costello CE. 2003. Elimination of oxidative degradation during the per-*O*-methylation of carbohydrates. J Am Chem Soc. 125:16213–16219.

Ciucanu I, Kerek F. 1984. A simple and rapid method for the permethylation of carbohydrates. Carbohydr Res. 131:209–217.

Dell A, Morris HR. 2001. Glycoprotein structure determination by mass spectrometry. Science. 291:2351–2356.

Dell A, Khoo K-H, Panico M, McDowell RA, Etienne AT, Reason AJ, Morris HR. 1993. In: Fukuda M, Kobata A, editors. Glycobiology: a practical approach. Oxford: Oxford University Press; pp. 187–222.

Garozzo D, Spina E, Sturiale L, Montaudo G, Rizzo R. 1994. Quantitative determination of β(1-2) cyclic glucans by matrix-assisted laser desorption mass spectrometry. Rapid Commun Mass Spectrom. 8:358–360.

Hakomori S. 1964. A rapid permethylation of glycolipid, and polysaccharide catalyzed by methylsulfinyl carbanion in dimethyl sulfoxide. J Biochem (Tokyo). 55:205–208.

Hakomori S. 2002. Glycosylation defining cancer malignancy: new wine in an old bottle. Proc Natl Acad Sci USA. 99:10231–10233.

Harazono A, Kawasaki N, Kawanishi T, Hayakawa T. 2005. Site-specific glycosylation analysis of human apolipoprotein B100 using LC/ESI MS/MS. Glycobiology. 15:447–462.

Harmon BJ, Gu X, Wang DI. 1996. Rapid monitoring of site-specific glycosylation microheterogeneity of recombinant human interferon-gamma. Anal Chem. 68:1465–1473.

Harvey DJ. 1993. Quantitative aspects of the matrix-assisted laser desorption mass spectrometry of complex oligosaccharides. Rapid Commun Mass Spectrom. 7:614–619.

Harvey DJ. 1999. Matrix-assisted laser desorption/ionization mass spectrometry of carbohydrates. Mass Spectrom Rev. 18:349–450.

Helenius A, Aebi M. 2004. Roles of *N*-linked glycans in the endoplasmic reticulum. Annu Rev Biochem. 73:1019–1049.

Huddleston MJ, Bean MF, Carr SA. 1993. Collisional fragmentation of glycopeptides by electrospray ionization LC/MS and LC/MS/MS: methods for selective detection of glycopeptides in protein digests. Anal Chem. 65: 877–884.

Imre T, Schlosser G, Pocsfalvi G, Siciliano R, Molnar-Szollosi E, Kremmer T, Malorni A, Vekey K. 2005. Glycosylation site analysis of human alpha-1-acid glycoprotein (AGP) by capillary liquid chromatography-electrospray mass spectrometry. J Mass Spectrom. 40:1472–1483.

Jefferis R. 2005. Glycosylation of recombinant antibody therapeutics. Biotechnol Prog. 21:11–16.

Kang P, Mechref Y, Klouckova I, Novotny MV. 2005. Solid-phase permethylation of glycans for mass spectrometric analysis. Rapid Commun Mass Spectrom. 19:3421–3428.

Karlsson NG, Wilson NL, Wirth HJ, Dawes P, Joshi H, Packer NH. 2004. Negative ion graphitised carbon nano-liquid chromatography/mass spectrometry increases sensitivity for glycoprotein oligosaccharide analysis. Rapid Commun Mass Spectrom. 18:2282–2292.

Kawasaki N, Ohta M, Hyuga S, Hashimoto O, Hayakawa T. 1999. Analysis of carbohydrate heterogeneity in a glycoprotein using liquid chromatography/mass spectrometry and liquid chromatography with tandem mass spectrometry. Anal Biochem. 269:297–303.

Krokhin O, Ens W, Standing KG, Wilkins J, Perreault H. 2004. Site-specific *N*-glycosylation analysis: matrix-assisted laser desorption/ionization quadrupole-quadrupole time-of-flight tandem mass spectral signatures for recognition and identification of glycopeptides. Rapid Commun Mass Spectrom. 18:2020–2030.

Lattová E, Kapková P, Krokhin O, Perreault H. 2006 Method for investigation of oligosaccharides from glycopeptides: direct determination of glycosylation sites in proteins. Anal Chem. 78:2977–2984.

Lemoine J, Chirat F, Domon B. 1996. Structural analysis of derivatized oligosaccharides using postsource decay matrix-assisted laser desorption/ionization mass spectrometry. J Mass Spectrom. 31:908–912.

Liu J, Volk KJ, Kerns EH, Klohr SE, Lee MS, Rosenberg IE. 1993. Structural characterization of glycoprotein digests by microcolumn liquid chromatography-ionspray tandem mass spectrometry. J Chromatogr. 632:45–56.

Mechref Y, Novotny MV. 2002. Structural investigations of glycoconjugates at high sensitivity. Chem Rev. 102:321–369.

Natsuka S, Hase S. 1998. Analysis of *N*- and *O*-glycans by pyridylamination. Methods Mol Biol. 76:101–113.

Naven TJ, Harvey DJ. 1996. Effect of structure on the signal strength of oligosaccharides in matrix-assisted laser desorption/ionization mass spectrometry on time-of-flight and magnetic sector instruments. Rapid Commun Mass Spectrom. 10:1361–1366.

Naven TJ, Harvey DJ, Brown J, Critchley G. 1997. Fragmentation of complex carbohydrates following ionization by matrix-assisted laser desorption with an instrument fitted with time-lag focusing. Rapid Commun Mass Spectrom. 11:1681–1686.

Royle L, Radcliffe CM, Dwek RA, Rudd PM. 2006. Detailed structural analysis of *N*-glycans released from glycoproteins in SDS-PAGE gel bands using HPLC combined with exoglycosidase array digestions. In: Brockhausen-Schutzbach I, editor. Glycobiology protocols. Methods in molecular biology. Vol. 347. Totowa (NJ): Humana Press; pp. 125–144.

Sheeley DM, Reinhold VN. 1998. Structural characterization of carbohydrate sequence, linkage, and branching in a quadrupole Ion trap mass spectrometer: neutral oligosaccharides and *N*-linked glycans. Anal Chem. 70: 3053–3059.

Spik G, Bayard B, Fournet B, Strecker G, Bouquelet S, Montreuil J. 1975. Studies on glycoconjugates. LXIV. Complete structure of two carbohydrate units of human serotransferrin. FEBS Lett. 50:296–299.

Sutton CW, O'Neill JA, Cottrell JS. 1994. Site-specific characterization of glycoprotein carbohydrates by exoglycosidase digestion and laser desorption mass spectrometry. Anal Biochem. 218:34–46.

Tajiri M, Yoshida S, Wada Y. 2005. Differential analysis of site-specific glycans on plasma and cellular fibronectins: application of a hydrophilic affinity method for glycopeptide enrichment. Glycobiology. 15: 1332–1340.

Takahashi N, Ishii I, Ishihara H, Mori M, Tejima S, Jefferis R, Endo S, Arata Y. 1987. Comparative structural study of the *N*-linked oligosaccharides of human normal and pathological immunoglobulin G. Biochemistry. 26:1137–1144.

Takahashi N. 1996. Three-dimensional mapping of *N*-linked oligosaccharides using anion-exchange, hydrophobic and hydrophilic interaction modes of high-performance liquid chromatography. J Chromatogr A. 720:217–225.

Tang H, Mechref Y, Novotny MV. 2005. Automated interpretation of MS/MS spectra of oligosaccharides. Bioinformatics. 21 Suppl 1:i431–i439.

Taniguchi N, Ekuni A, Ko JH, Miyoshi E, Ikeda Y, Ihara Y, Nishikawa A, Honke K, Takahashi M. 2001. A glycomic approach to the identification and characterization of glycoprotein function in cells transfected with glycosyltransferase genes. Proteomics. 1:239–247.

Viseux N, Hronowski X, Delaney J, Domon B. 2001. Qualitative and quantitative analysis of the glycosylation pattern of recombinant proteins. Anal Chem. 73:4755–4762.

Wada Y, Tajiri M, Yoshida S. 2004. Hydrophilic affinity isolation and MALDI multiple-stage tandem mass spectrometry of glycopeptides for glycoproteomics. Anal Chem. 76:6560–6565.

Zaia J. 2004. Mass spectrometry of oligosaccharides. Mass Spectrom Rev. 23: 161–227.

Zamfir A, Konig S, Althoff J, Peter-Katalinc J. 2000. Capillary electrophoresis and off-line capillary electrophoresis-electrospray ionization quadrupole time-of-flight tandem mass spectrometry of carbohydrates. J Chromatogr A. 895:291–299.

Journal of Organ Dysfunction, 2007; 3: 164–182

informa
healthcare

REVIEW ARTICLE

Study of hepatocytes using RNA interference

SHINGO NIIMI[1], MIZUHO HARASHIMA[2], MASASHI HYUGA[1] and TERUHIDE YAMAGUCHI[1]

[1]*Division of Biological Chemistry and Biologicals, National Institute of Heath Sciences, Tokyo, Japan, and* [2]*Department of Nutrition and Physiology, Nihon University College of Bioresource Sciences, Fujisawa, Japan*

Abstract

RNA interference (RNAi) is the process of sequence-specific gene silencing, initiated by small double-stranded RNA homologous in sequence to the target gene. Various factors involved in the regulation of hepatocyte function have been identified using RNAi, indicating that RNAi is a useful strategy for characterization. There has been some success in treating experimental liver dysfunction using RNAi in several model systems, suggesting a promising new therapeutic strategy. A number of groups have also demonstrated that RNAi can interfere with hepatitis C virus and hepatitis B virus gene expression and replication in several model systems, suggesting a new approach for the treatment of these viral diseases. This review summarizes studies of hepatocytes using RNAi.

Key words: *Hepatitis B virus, hepatitis C virus, hepatocyte, RNA interference, short hairpin RNA, small interfering RNA*

Introduction

RNA interference (RNAi) is a process by which double-stranded RNA (dsRNA) triggers sequence-specific silencing of homologous genes (1). This process is evolutionarily conserved through a variety of eukaryotic organisms (2,3). The process is initiated by the RNase III-like nuclease Dicer, which promotes progressive cleavage of long dsRNAs into 21–27-nucleotide (nt) short interfering RNA (siRNA) with two-nt 3′-overhangs. Subsequently, the siRNA unwinds and binds to an activated RNAi-induced silencing complex. Single-stranded (ss) siRNAs then bind to target sequences based on sequence complementarity, resulting in cleavage of the target sequence (4–10). Although first discovered in the worm Caenorhabditis elegans, it was demonstrated soon after that RNAi can be induced in various mammalian cells by introducing synthetic 21-nt siRNA to obtain strong and specific suppression (knockdown) of gene expression (11). Exposure to dsRNAs >30 bp in length induces an antiviral interferon response that generally represses mRNA translation through the activation of dsRNA-dependent protein kinase (PKR) and 2′,5′-oligoadenylate synthetase (2′,5′-OAS) (12,13). This kind of RNAi is highly sequence-specific, with even a single mismatch between the siRNA and its target sequence being able to dramatically decrease the efficacy of RNA degradation. Systems for stable and continuous expression of short hairpin RNA (shRNA) and duplex siRNA transcribed in vitro and in vivo from DNA templates also suppress gene expression in mammalian cells (14–17). From a practical perspective, RNAi has become a powerful non-destructive, non-mutating tool for the analysis of gene function in different living systems (18–20) and one that holds great promise for the treatment of many infectious diseases and cancers (21–24).

In this review, efforts to identify factors involved in the regulation of hepatocyte function, and to treat experimental liver failure, hepatitis C virus (HCV), and hepatitis B virus (HBV) disease using RNAi are summarized.

Correspondence: Shingo Niimi, PhD, Division of Biological Chemistry and Biologicals, National Institute of Health Sciences, 1-18-1 Kamiyoga, Setagaya-ku, Tokyo 158-8501, Japan. Fax: +81 3 3700 9347. E-mail: niimi@nihs.go.jp

ISSN Print 1747-1060 ISSN Online 1747-1079
DOI: 10.1080/17471060701286559

Identification of factors involved in the regulation of hepatocyte function using RNAi

Various factors involved in the regulation of hepatocyte function using RNAi are described below and summarized in Table I.

Annexin A3

Small hepatocytes are a minor subpopulation of cells with high replication potential in defined media (25–27). After 1 day of culture, small hepatocytes express universal hepatocyte markers, differentiating into cells expressing differentiated hepatocyte marker or biliary cell marker protein (28). The molecular mechanism regulating these characteristic phenotypes is yet to be elucidated. Niimi et al. (29) attempted to identify proteins specifically expressed in isolated small, but not parenchymal, isolated rat hepatocytes using a proteomic approach. Annexin A3 was only expressed in the small rat hepatocytes. Annexin A3 siRNA inhibited stimulation of DNA synthesis by hepatocyte growth factor (HGF) and epidermal growth factor (EGF), suggesting that annexin A3 is necessary for DNA synthesis in cultured parenchymal rat hepatocytes (30).

Coactivator-associated arginine methyltransferase

De novo glucose production, e.g. gluconeogenesis, represents a key feature of hepatic metabolism under fasting conditions to maintain blood glucose levels and energy substrates for brain function (31). Phosphoenolpyruvate carboxikinase (PEPCK) and glucose-6-phosphatase (G6Pase) genes have been identified as the rate-limiting steps in the gluconeogenic pathways. Transcription of these genes is stimulated by glucagon via intracellular cyclic adenosine monophosphate/protein kinase A (PKA) (31–33). Coactivator-associated arginine methyltransaferase (CARM1) was originally identified as a co-factor for the estrogen receptor, working in combination with members of the p160 family of nuclear receptor co-factors (e.g. steroid receptor coactivator-1/TIF2/glucocorticoid receptor interaction protein 1), as well as the cAMP-responsive element binding factor-binding protein CBP/P300 (34,35).

CARM1 siRNA inhibited PKA-induced PEPCK and G6Pase promoter activities in HepG2 cells, suggesting that CARM1 plays a role in the stimulation of PEPCK and G6Pase gene expression by PKA (36).

Aryl hydrocarbon receptor

It has been suggest in numerous reports (37–44) that 2,3,7,8-tetrachlorodibenzo-*p*-dioxin (TCCD) promotes Fas-mediated apoptosis. The aryl hydrocarbon receptor (AhR) is a cytosolic, ligand-activated transcription factor that regulates the expression of several genes in response to polycyclic and halogenated aromatic hydrocarbon ligands, such as TCCD (45,46).

Table I. Regulation of hepatocyte function using RNAi.

Target gene	Regulation of hepatocyte function	Reference
Annexin A3	Inhibition of Stimulation of DNA synthesis by HGF and EGF	30
CARM1	Inhibition of PKA-induced PEPCK and G6Pase promoter activities	36
AhR	Protection of Jo2-induced lethality	47
MIZ-1	Inhibition of T113242-dependent activation of LDL gene and cell growth	49
LRH-1	Down-regulation of APOA1 gene expression	51
GATA-4	Inhibition of Epo gene expression	59
FOXO1	Decrease of reporter activity derived from CAR	80
ARH	Reduction of LDL internalization	85
Pim-3	Attenuation of proliferation rates, stimulation of cell death	90
GR, MR	Abolition of UDCA protection against TGF-β1-mediated apoptosis, decrease of protective effect of UDCA in TGF-β1-associated caspase activation and TGF-β1-induced E2F-l/Mdm/p53 apoptotic pathway	110
cFLIP	Reversion of anti-apoptotic effect of Dex against TNF-α+Actinomycin D-induced apoptosis	117
MLCK	Inhibition of DNA replication, expression of cdk1 and phosphorylation of p70S6K induced by EGF	121
ERK2	Inhibition of phosphorylation of p70S6K induced by EGF	121
p70S6K	Suppression of stimulation of DNA synthesis by EGF	121
EndoG	Suppression of decrease in TUNEL-positive nuclei	132
DNMT3B	Upregulation or downregulation of some important developmental genes and tumor-related genes	135
PTEN	Prevention of TNF-activated cell death signaling pathways, prevention of promotion of Bax-induced mitochodrial injury by TNF, prevention of induction of cell death by ethanol	147
TLR3, TRIF	Inhibition of induction of IFN-β promoter activity and ISG56mRNA transcription in response to Poly (I-C)	158
RIG-1	Inhibition of induction of IFN-β, NF-κB-dependent PRDII promoters, inhibition of transcription of ISG mRNA in response to Sen V	158
TLR3	Override of induction of IFN-β and cell cycle delay	175

Park et al. (47) investigated the role of AhR in Fas-mediated apoptosis by using adenovirus (Ad) expressing siRNA against AhR. Treatment of mice with siRNA protects against Jo2-induced lethality. Furthermore, AhR expression in primary hepatocytes from $AhR^{-/-}$ mice increases Fas ligand-induced apoptosis. These findings indicate that AhR predisposes hepatocytes to Fas-mediated apoptosis and subsequent lethality in animals.

Myc-interacting protein 1

Myc-interacting protein 1 (MIZ-1) was identified by virtue of its ability to bind to Myc.

MIZ-1 is sequestered in the cytoplasm by association with microtubules. Upon drug-induced microtubule depolymerization, MIZ is free to enter the nucleus where it binds to target sequences, such as low-density lipoprotein receptor (LDLR) gene promoter, and activates transcription (48).

Using the microtubule disrupting agent T113242, Ziegelbauer et al. (49) demonstrated that MIZ-1 siRNA inhibited T113242-dependent activation of the LDL gene in HepG2 cells, inhibiting cell growth.

Liver receptor homolog-1

The orphan nuclear receptor liver receptor homolog-1 (LRH-1) regulates the scavenger receptor class B type 1 gene (50) that mediates selective uptake of high-density lipoprotein (HDL) and plays a key role in reverse cholesterol uptake. Apolipoprotein A1 (APOA1), the major protein component of HDL, plays a role in reverse cholesterol transport.

Delerive et al. (51) demonstrated that LRH-1 siRNA downregulated APOA1 gene expression in HepG2 cells, suggesting that LRH-1 plays a role in the stimulation of APOA1 gene expression.

GATA-4

Erythropoietin (Epo) production sites developmentally change and switch from the fetal liver to adult kidney (52,53). GATA transcriptional factors belong to the family of zinc DNA-binding proteins and play critical roles in cell growth and differentiation (54,55). GATA-4, one of six members of the GATA family, is expressed in the liver during murine embryogenesis (56). Expression of GATA-4 is detectable late in gestation only in endothelial/epithelial cells surrounding the hepatic vessels. In a recent study (57) it was demonstrated that GATA-4 cooperates with hepatocyte nuclear factor-3 to stimulate the albumin gene in liver progenitor cells. Hep3B is a hepatoma cell line similar to fetal hepatocytes and is generally accepted as a good model for hepatic Epo gene regulation (58)

Dame et al. (59) demonstrated that GATA-4 shRNA inhibited Epo gene expression, suggesting that GATA-4 plays a critical role in Epo gene regulation in Hep3B cells.

FOXO1

FOXO1, a forkhead transcription factor, activates gluconeogenic genes by binding to an insulin response element (IRS) located on those genes (60–64). Insulin phosphorylates FOXO1 via a phosphatidylinositol 3-kinase–Akt pathway (60,65, 66) and inactivates FOXO1 by decreasing the binding affinity of FOXO1 to IRS and/or exporting FOXO1 from the nucleus (67–70). Insulin represses the induction of drug-metabolizing enzymes by certain drugs in diabetic livers (71–73) and rat primary hepatocytes (74–76). In contrast, the nuclear receptor CAR plays a central role in the induction of drug-metabolizing enzymes, such as cytochrome P450s, by certain drugs (77–79).

Kodama et al. (80) demonstrated that FOXO1 siRNA decreased reporter activity derived from CAR in HepG2 cells, suggesting that FOXO1 may play a role in regulating CAR-mediated transactivation in HepG2 cells.

Autosomal recessive hypercholesterolemia

LDLR plays a pivotal role in the regulation of cholesterol metabolism (81). LDLR is a ubiquitous cell surface glycoprotein which is able to bind LDL, the major cholesterol transport vesicle in plasma. The autosomal recessive hypercholesterolemia (ARH) protein contains an ≈130-residue phosphotyrosine-binding domain evolutionarily related to other adaptor proteins. These adaptor proteins, including ARH, bind the conserved sequence motif NPXY located in the cytoplasmic domain of various cell surface receptors and mediate several functions, including trafficking and endocytosis. The LDLR cytoplasmic tail contains a single NPXY motif required for clustering and endocytosis of the receptor in fibroblasts. Transformed lymphocytes and monocyte-derived macrophage obtained from ARH patients are unable to take up and degrade ^{125}I-LDL (82–84), suggesting that ARH is required for efficient endocytosis of LDL in these cells.

A quantitative immunofluorescence analysis performed by Sirinian et al. (85) indicated that ARH siRNA causes a reduction in LDL internalization, suggesting that ARH is an endocyte-sorting adaptor that actively participates in internalization of the LDL–LDLR complex.

Pim-3

Among human cancers, the greatest number of deaths result from hepatocellular carcinoma (HCC). Most cases of HCC arise from chronic infection with human HBV or HCV (86). Host responses are assumed to be involved in the development of HCC, as these viruses lack apparent oncogenes and infected patients develop HCC after suffering from chronic hepatitis-related pathology (87,88).

Nakamoto et al. (89) used a mouse model of HCC, established using an HBV surface antigen (HBsAg) transgenic mouse, to compare gene expression in the non-tumor portion of this disease, examining pre-malignant lesions and normal tissue (90). Gene expression of Pim-3, which is involved in EWS/ETS-mediated malignant transformation of NIH 3T3 cells (91), was enhanced in pre-malignant regions. siRNA against Pim-3 attenuated proliferation rates and caused cell death in HuH7 cells, suggesting that Pim-3 can cause autonomous cell proliferation or prevent apoptosis in HuH7 cells.

Glucocorticoid receptor and mineralocorticoid receptor

E2F-1 is the best-characterized member of the E2F family of transcriptional factors, regulating a number of genes involved in apoptosis (92,93). Unbound E2F-1 modulates transforming growth factor (TGF)-β1-induced apoptosis in hepatic cells (94–96). The ability of E2F-1 to promote apoptosis involves stabilization of tumor suppressor protein p53 via transcription of $p14^{ARF}$, which markedly inhibits the p53 repressor Mdm-2 (93,94). Ursodeoxycholic acid (UDCA) interrupts the apoptotic pathway by interfering with mitochondrial pathways in both hepatic and non-hepatic cells (97–100), and interfering with the E2F-1/p53 apoptotic pathway (94). UDCA also modulates activation of glucocorticoid receptor (GR) (101), probably by interaction with distinct regions of its ligand-binding domain, thus suppressing, for example, nuclear factor (NF)-κB-dependent transcription (102). Dexamethasone (Dex), a strong activator of GR, prolongs cell viability, inhibits the development of apoptotic morphology, and stabilizes the expression of procaspase-3 in both human and rat hepatocytes (103), plus inhibiting TGF-β1-induced apoptosis in rat hepatoma cells (104). Mineralocorticoid receptor (MR) also has a predominantly anti-apoptotic role in several neuronal systems (105–109).

Sola et al. (110) demonstrated that both GR and MR siRNAs abolished UDCA protection against TGF-β1-mediated apoptosis. Both GR and MR siRNAs also decreased the protective effect of UDCA in TGF-β1-associated caspase activation and the TGF-β1-induced E2F-1/Mdm/p53 apoptotic pathway. These results demonstrate that UDCA protects against apoptosis through GR and MR, and that the E2F-1/Mdm/p53 apoptotic pathway appears to be a prime target for UDCA-induced GR and MR activation.

FLICE inhibitory protein

Hepatocyte apoptosis can be initiated by exposure to toxic substances or ligation of members of the death receptor family, including tumor necrosis factor (TNF)-α receptor (TNF-R) and Fas (111). Dex inhibits apoptosis in primary human and rat hepatocytes (103). Although several sets of genes have been characterized as being involved in the anti-apoptotic effect of Dex in spontaneous apoptosis of cultured primary hepatocytes (112), the mechanism behind the anti-apoptotic effect of Dex has rarely been investigated in death receptor-mediated apoptosis. FLICE inhibitory protein (cFLIP) is a cellular inhibitor for caspase-8 activation in death receptor-induced apoptosis (113), inhibiting apoptosis induced by death receptor-activating ligands, such as TNF-α, FasL (114), and TNF-related apoptosis-inducing ligand (114–116).

Oh et al. (117) found that Dex upregulated cellular cFLIP expression. siRNA against cFLIP reversed the anti-apoptotic effect of Dex by increasing caspase-8 activation in TNF-α + actinomycin D-induced hepatocyte apoptosis. These results indicate that Dex exerts a protective role in death receptor-induced hepatocyte apoptosis by upregulating cFLIP expression.

Myosin light-chain kinase, extracellular signal-regulated kinase-2 and p70S6K

Inhibition of myosin light-chain kinase (MLCK) blocks DNA synthesis in hepatocytes cultured on high-density fibronectin (118). p70S6K has been implicated in the regulation of hepatocyte proliferation, and extracellular signal-regulated kinase (ERK) has been reported to phosphorylate p70S6K in hepatocytes (119,120).

Bessard et al. (121) investigated the role of MLCK in cell-cycle progression in cultured rat hepatocytes by using siRNAs against MLCK, ERK2, and p70S6K. MLCK siRNA inhibited DNA replication and the expression of cdk1, a marker of S phase progression, and cyclin E, a major player in initial S progression in EGF-treated cells. ML7, an inhibitor of MLCK, inhibited cyclin D1, an important regulator of late G1 phase progression at the mRNA level. Both MLCK and ERK2 siRNAs inhibited

phosphorylation of p70S6K induced by EGF. p70S6K siRNA suppressed stimulation of DNA synthesis by EGF. These results underline the fact that there is an MLCK-dependent restriction point in G1/S transition which occurs downstream of ERK2 by means of regulation of p70S6K activation.

Endonuclease G

Apoptosis is a major cellular response against oxidative stress, the mechanisms of which have been extensively discussed (122–127). Inhibition of catalase and glutathione peroxidase activities by 3-amino-1,2,4-triazole (ATZ) and mercaptosuccinic acid (MS) caused sustained endogenous oxidative stress and apoptotic cell death without caspase-3 activation, respectively in rat primary hepatocytes (128,129). Endonuclease G (EndoG), an executive cause of DNA fragmentation, has been shown to be caspase-independently translocated from mitochondria to nuclei in response to apoptotic stimuli, with subsequent induction of nucleosomal DNA fragmentation (130,131).

Ishihara et al. (132) demonstrated that EndoG siRNA significantly suppressed decreases in terminal deoxynucleotide transferase-mediated dUTP nick-end labeling (TUNEL)-positive nuclei, indicating that EndoG is involved in DNA fragmentation induced by ATZ and MS.

De novo methyltransferase 3B

De novo methyltransferase 3B (DNMT3B) is one of several DNMT3 isoforms involved in establishing genomic methylation patterns (133,134). Expression of DNMT3B was minimally observed in some non-tumor livers and normal liver cell lines, but was much higher in HCCs and in HCC cell lines, suggesting that DNMT3B has a role relevant to liver cancer.

Jun et al. (135) investigated the influence of DNMT3B in gene expression by using siRNA against DNMT3B in the human HCC cell line SMMC-7721. Microarray analysis identified 26 down- and 115 upregulated genes in cells treated with DNMT3B siRNA. These genes included important developmental and tumor-related genes, such as SNCG, NOTCH1, MBD3, WNT11, MAOA, and FACL4.

Phosphate and tensin homolog deleted from chromosome 10

TNF is a central agent in the genesis of alcoholic liver disease (136–140). When hepatocytes are exposed to ethanol, they exhibit increased sensitivity to TNF-induced cell death (141,142). Activated Akt acts as an inhibitor of apoptosis (143–145) and phosphatidylinositol 3,4,5-triphosphate (PIP_3) is necessary for its activation. TNF receptor (TNFR) stimulates Akt activation by activating phosphatidylinositol 3-kinase, phosphorylating PIP_2 to generate PIP_3. When primary hepatocytes and the hepatoma cell line HepG2E47 are exposed to ethanol, these cells exhibit a decrease in stimulation of Akt activity by TNF (146). In contrast, phosphate and tensin homolog deleted from chromosome 10 (PTEN) is a tyrosine phosphatase with dual protein and lipid phosphatase activity. PTEN recognizes PIP_3 as a substrate and removes the D3 phosphate from the inositol ring, which is likely to cause a decrease in the concentration of PIP_3 and thus inhibit TNF-stimulated Akt activity.

Shulga et al. (147) investigated the role of PTEN in ethanol-induced signaling pathways that elicit sensitization to TNF cytotoxicity using siRNA against PTEN. PTEN expression increased in ethanol-exposed HepG2E47 cells. PTEN siRNA prevented TNF-activated cell death signaling pathways, such as p38 activation, apoptosis signaling kinase 1 phosphorylation, and translocation of Bax from cytosol to the mitochondria in ethanol-exposed cells. PTEN siRNA also prevents TNF from promoting Bax-induced mitochondrial injury, such as the loss of cytochrome C from mitochondria and localization to the cytosol, plus cell death, in ethanol-exposed cells. These findings indicate that PTEN is involved in the increased sensitivity of ethanol-exposed cells to TNF-induced cytotoxicity.

Toll-like receptor-3, Toll-interleukin-1 receptor domain-containing adaptor-inducing interferon-β and retinoic acid-inducible gene 1

Innate cellular antiviral defenses are likely to influence the outcome of infections by many human viruses. Toll-like receptors (TLRs) are a class of pathogen-associated molecular partners that detect infection by many types of pathogen, including viruses (148). TLR3 is engaged specifically by dsRNA present either in the viral genome or generated during viral replication, and is involved in cellular recognition of RNA viruses and the induction of type 1 interferon (IFN) responses (149). TLR-3 signaling requires the adaptor protein Toll-interleukin (IL)-1 receptor (TIR) domain-containing adaptor-inducing IFN-β (TRIF)/TIR domain-containing adaptor molecule 1 (TICAM1) (150–153). However, it has been indicated in several recent studies (154–156) that viral infection can also activate the host response through TLR3-independent pathways. Retinoic acid-inducible gene

1 (RIG-1) is a cytoplasmic RNA helicase that putatively binds viral dsDNA within its helicase domain, resulting in activation of IFN regulatory factor 3 and NF-κB (157). Although the liver is a very important site of persistent viral infection in humans, very little is known about how these pathways function, specifically in hepatocytes.

Li et al. (158) investigated antiviral signaling pathways active in the hepatocyte-derived cell line PH5CH8 using siRNAs against TLR3, TRIF, and RIG-1. PH5CH8 cells are derived from non-neoplastic hepatocytes transformed with T antigen from non-neoplastic liver tissue of a HCV-related HCC patient (159,160). Poly (I-C) activated the IFN-β promoter, resulting in robust expression of IFN-stimulated genes (ISG) in the cells. TLR3 siRNA or TRIF siRNA inhibited induction of IFN-β promoter activity and ISG56 mRNA transcription in response to Poly (I-C), but not Sendai virus (Sen V). RIG-1 siRNA inhibited induction of IFN-β, NF-κB-dependent PRDII promoters, and transcription of ISG mRNA in response to Sen V. However, RIG-1 siRNA did not inhibit Poly (I-C) induction of ISG56 transcription. These findings indicate that hepatocytes contain two distinct antiviral signaling pathways leading to expression of type 1 IFNs, one dependent on TLR3 and the other on RIG-1, with little evidence of significant cross-talk between them.

NS5B

Although persistent infection with HCV is a major cause of various human liver diseases, as described below, the molecular mechanisms remain elusive. Unregulated cell-cycle progression may be a cause of malignant transformation of normal cells. Inhibition of cell-cycle progression through the S phase may cause replication errors during DNA replication, inducing genomic instability and malignant transformation. Therefore, it is important to clarify the effect of HCV proteins on cell-cycle progression in order to determine molecular mechanisms underlying the pathogenesis of HCV. Although it was suggested in a number of previous reports (161–164) that several HCV proteins are involved in modulating cell-cycle progression, the conclusions of those studies are still being debated (165–171). However, several findings (159, 172–174) indicate that the PH5CH8 cell line described above is more relevant for studying the role of HCV proteins during hepatocarcinogenesis.

Naka et al. (175) investigated the effect of HCV NS5B, an RNA-dependent RNA polymerase, on the pathogenesis of HCV using siRNA against TLR3 in the PH5CH8 cell line. Infection with a retroviral vector encoding HCV NS5B delayed cell-cycle progression through the S phase and promoted IFN-β production in the PH5CH8 cell line, and an anti-IFN-β antibody restored the cell-cycle delay. TLR3 siRNA overrode the induction of IFN-β and the cell-cycle delay. These findings indicate that NS5B delays cell-cycle progression by inducing IFN-β through activation of the TLR signaling pathway.

Treatment of experimental liver dysfunction by RNAi

RNAi targeting the key factors involved in the development of liver dysfunction can effectively treat experimentally induced dysfunction in several model systems. Several of these findings are described below and summarized in Table II. RNAi represents a promising new strategy for the treatment of liver dysfunction.

Rejection after hepatocyte transplantation/Fas

Fas-mediated apoptosis has also been implicated in hepatocyte apoptosis upon allogenic hepatocyte transplantation (176). Blockade of Fas and Fas ligand interactions promotes repopulation of allogenic liver cells in recipient spleen (177).

Wang et al. (178) investigated the protective effects of siRNA against Fas on allogenic hepatocytes transplanted into mouse spleen. Transplantation of

Table II. Treatment of experimental liver dysfunction using RNAi.

Target gene	Treatment of liver dysfunction	Model	Reference
Fas	Decrease of apoptosis, improvement of decrease of survival	Rejection after hepatocyte transplantation	178
Caspase 8	Prevention of apoptosis, reduction of liver damage, improvement of decrease of survival	Fas-mediated ALF	184
TGF-βII	Suppression of expression of several TGF-β-responsive genes, prevention of cell damage, prevention of release of aminotransferases, improvement of decrease of survival	Fas-mediated acute liver injury and ALF	188
Fas	Abrogation of necrosis and inflammatory infiltration, prevention of elevation of serum transaminases, improvement of decrease in survival	Fas-mediated liver failure and fibrosis	194

hepatocytes treated with Fas siRNA into recipient spleen after 21 days resulted in a decrease in apoptosis of ≈50% and increased survival of transplanted hepatocytes approximately twofold. These results suggest that Fas silencing by RNAi holds promise for inhibiting acute rejection after hepatocyte transplantation.

Fas-mediated acute liver failure/caspase-8

Acute liver failure (ALF) is a dramatic clinical syndrome in which a previously normal liver fails within days or weeks and is associated with high mortality rates. In ALF, signals from death receptors, such as Fas (CD95), TNF-α, and TNF-related apoptosis-inducing ligand, trigger suicide pathways (179–181), leading to the activation of caspase cascades that subsequently induce the apoptotic death of hepatocytes. Consequently, an attractive strategy to treat patients with ALF would be to inhibit death receptor-mediated apoptosis to maintain liver function and save the organ.

Zender et al. examined the efficacy of siRNA against caspase 8, a key enzyme in death receptor-mediated apoptosis (182,183), to protect against ALF using different mouse models (184). Systematic application of caspase 8 siRNA prevents Fas (CD95)-mediated apoptosis of hepatocytes. Protection of hepatocytes by caspase 8 siRNA results in reduced liver damage after application of activating anti-Fas (CD95) antibody (Jo2) or Ad-expressing Fas ligand (AdFasL). Survival improved after delayed treatment of mice with caspase 8 siRNA following administration of AdFasL or Ad wild type. These findings demonstrate the therapeutic potential of RNAi targeting caspase 8 in ALF.

Fas-mediated ALF and ALF/ TGF-β receptor II

In the liver, TGF-β plays an essential role in hepatocyte apoptosis, growth inhibition, and the progression of fibrogenesis. The pathology underlying ALF involves overefficient apoptosis and the inhibition of hepatocyte regeneration associated with TGF-β signaling (185,186). TGF-β receptor II (TGF-βR-II) is considered a key target for interfering with TGF-β signaling (187). However, the potential use of in vivo RNAi in therapy and analytical activity by suppressing TGF-βR-II in the TGF-β signaling pathway has not yet been established or documented.

To approach this problem, Mizuguchi et al. (188) investigated the effect of the shRNA against TGF-βR-II using hepatocyte injury in mouse BNL, CL.2 cells, and liver injury models. TGF-βR-II shRNA suppressed the activation of SMAD2 and the induction of several TGF-β-responsive genes by TGF-β1 in the mouse cells. TGF-βR-II shRNA suppressed inhibition of cell proliferation and stimulation of apoptosis by TGF-β1. In a mouse acute liver injury model induced by Jo2 antibody, TGF-β-RII shRNA suppressed several TGF-β-responsive genes, prevented cell damage, and prevented the release of aminotransferases from damaged hepatocytes. In a survival study with Fas-mediated ALF, TGF-β-RII shRNA protected mice from death. These findings indicate that the use of shRNA targeting TGF-βR-II has great potential as an analytic tool for TGF-βR-II in TGF-β signaling and gene-specific therapeutics for human disorders.

Fas-mediated liver failure and fibrosis/Fas

Fas-mediated hepatocyte apoptosis is implicated in a broad spectrum of liver diseases, including the development of liver fibrosis in chronic hepatitis (189–192). Fas-deficient lpr mice survive challenge with factors that induce fulminant hepatitis in normal mice (190,193), and show reduced fibrosis after chronic hepatic insult (191).

Song et al. (194) investigated the effect of siRNA against Fas for protecting mice from liver failure and fibrosis in two models of autoimmune hepatitis. Hepatocytes isolated from mice treated with Fas siRNA were resistant to apoptosis when exposed to Jo2 in vitro or co-cultured with hepatic mononuclear cells harvested from concanavalin A (ConA)-treated mice. Hepatocytes from mice treated with Fas siRNA were resistant to cytolysis by hepatic mononuclear cells from ConA-treated mice. Treatment with Fas siRNA 1 day before ConA treatment abrogated hepatocyte necrosis and inflammatory infiltration, as well as almost completely preventing elevation of serum transaminases. Treatment with Fas siRNA, beginning 1 week after the initiation of weekly ConA treatment, protected mice from liver fibrosis. In a more aggressive hepatitis model using a Fas-specific antibody, 82% of mice treated with Fas siRNA survived for 10 days, whereas all control mice died within 3 days. These results indicate that siRNA-directed Fas silencing may be of therapeutic value in preventing liver injury by protecting hepatocytes from cytotoxicity.

Inhibition of HCV gene expression and replication by RNAi

HCV is an enveloped virus with a ss 9.6-kb RNA genome of positive-stranded polarity (195). The 5′ non-translated region of the genome contains an internal ribosome entry site (IRES) that directs translation of a single long reading frame (196–198).

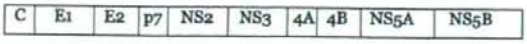

Fig. 1. Schematic representation of the HCV genome.

The HCV open reading frame (ORF) encodes a single polyprotein that is 3008–3037 amino acids in length and is post-translationally modified to produce at least 10 different proteins: core, the envelope proteins E1 and E2, p7, and the non-structural proteins NS2, NS3, NS4A, NS4B, NS5A, and NS5B (Fig. 1) (162,199). These viral proteins are not only involved in viral replication but may also affect a variety of cellular functions (162,200). Based on nt sequence comparisons, HCV genomes can be grouped into at least six genotypes, or clades, that differ from each other by 31–34%. Furthermore, several subtypes have been defined, with an nt sequence diversity of ≈20%. HCV has infected an estimated 170 million people worldwide, making it a global health problem (201). HCV is one of the main causes of liver-related morbidity and mortality; it establishes a persistent infection of the liver, leading to the development of chronic hepatitis, liver cirrhosis, and HCC (202). It is estimated that 40–60% of infected individuals progress to chronic liver disease, with many of these patients ultimately requiring liver transplantation (203). At present, HCV infections can be treated with IFN-β, either alone or in combination with ribavirin. Standard therapy has a poor response rate (204), and thus alternative therapeutic approaches for chronic HCV are needed. To overcome this situation, a number of groups have attempted to verify the usefulness of RNAi as a therapeutic tool in several model systems, as described below. The findings indicate that siRNA and shRNA against HCV interfere efficiently with HCV gene expression and replication.

McCaffrey et al. (205) investigated the effect of siRNA and plasmids expressing shRNA against HCV NS5B on the expression of an HCV NS5B fragment fused with luciferase RNA in mouse liver using hydrodynamic injection. Quantitative whole-body imaging showed that siRNA and shRNA decreased luciferase expression by 75% and 90%, respectively.

Wilson et al. (206) investigated the effect of siRNA on the expression of HCV-specific proteins and RNA synthesis in Huh cells containing an HCV subgenome replicon. siRNA against NS5b and NS3 inhibited expression of NS3 and NS5b protein and reduced HCV replicon RNA levels by >94%. These siRNAs protected native Huh7 cells from challenge with HCV replicon RNA by >95%. Treatment of the cells with the siRNAs was effective for >72 h, but the duration of RNAi treatment could be extended beyond 3 weeks through stable expression of complementary strands of siRNA under the control of two separate H1 promoters by using a vector. The vector-based siRNA protected native Huh7 cells from challenge with HCV replicon RNA by 70%.

Wilson et al. (207) wondered whether the small percentage of surviving Huh cells challenged with HCV replicon were resistant to RNAi in general or to the specific siRNA being used. After several treatments with a highly effective siRNA, growth of replicon RNAs resistant to subsequent treatment with the same siRNA was observed. Sequence analysis of the siRNA-resistant replicon showed the generation of point mutations within the siRNA target sequence. Use of a combination of two siRNAs severely limited escape mutant evolution.

Kapadia et al. (208) investigated the effect of siRNA, NS3-1948, and NS5B-6133 (named on the basis of their nt location in subgenomic replication) on ongoing HCV replication and protein expression in Huh7 cells that stably replicate HCV RNA. siRNAs decreased HCV replication ≈20-fold. The RNAi effect was effective for at least 6 days. siRNAs decreased NS3 and NS5B proteins on Day 4. The siRNAs induced several IFN-induced genes to a much lesser extent compared to IFN, suggesting that the inhibition of HCV replication was not due to dsRNA-induced activation of the IFN pathway. siRNAs did not affect the cell cycle, suggesting that inhibition of HCV replication was not due to an effect on cell-cycle progression.

Randall et al. (209) investigated the effect of siRNA against 5′ core and NS4B regions on the NS5B protein, as well as cytoplasmic replication of HCV RNA in Huh7.5 cells containing HCV-Con1 and HCV-C/LB. HCV-Con1 is a full-length genotype 1b replicon with a highly adaptive serine to isoleucine substitution at amino acid 2204 of the HCV polypeptide. This has previously been described as Con/F1-neo (S22041) (210). HCV-C/LB is a chimeric replicon in which Con1 sequences, including part of NS3, all of NS4A, -4B, and -5A, and part of NS5B, were replaced with the corresponding region from the genotype 1b LB strain. siRNA against the 5′ core region (siHCV) decreased NS5B protein to an undetectable level in HCV-Con1 and HCV-C/LB cells on Day 4. siRNA against the NS4B region also decreased the NS5B protein to an undetectable level in HCV-Con1 cells, but not in HCV-C/LB cells. siHCV decreased the HCV RNA level 80-fold at Day 4 in the HCV-Con1 cells, and this level was maintained after 4 days. siHCV decreased the number of NS5A staining cells by >99%. Randall et al. also assessed the efficacy of siHCV in clearing Huh7.5 cells of replicating full-length HCV. The measurement was based on the

phenomenon that the ability to form G418-resistant colonies depends on persistent expression of neomycin phosphotransferase from replicating HCV RNAs. siHCV decreased the formed G418-resistant colonies by 99.6%.

The 5′ untranslated region (UTR) and the upstream portion of the core region are the most conserved parts in the HCV genome, with an nt identity of 99.6% (211,212). Therefore, the 5′ UTR appears to be an ideal target for siRNA. Yokota et al. (213) investigated the effect of siRNA targeting the 5′ UTR on HCV IRES-mediated translation, HCV replication, and protein expression. siRNA decreased luciferase activity by 81% at a concentration of only 2.5 nM in Huh7 cells transiently transfected with an HCV IRS reporter gene vector. This vector expresses mRNA consisting of the HCV 5′ UTR and the upstream part of the core region, connected in-frame with the firefly luciferase (FL) gene as reporter. siRNA decreased luciferase activity, the non-structural viral proteins NS3, -4, and -5, and intracellular replication of HCV genome RNA in Huh7 cells stably expressing an HCV Feo replicon that expressed mRNA consisting of FL and NS3, -4, -5A, and -5B.

The high degree of sequence diversity between different HCV genotypes and the notoriously error-prone replication of HCV are the major problems in the development of siRNA-based gene therapies.

Kronke et al. (214) developed two alternative strategies to overcome these obstacles. In one approach, they used endoribonuclease-prepared siRNAs (esiRNAs) to simultaneously target multiple sites of the HCV genome and investigated the effect of esiRNAs on the replication of subgenomic and genomic HCV replicon in Huh cells transfected with HCV replicon encoding FL as a reporter. siRNAs directed against various regions of the HCV coding sequence as well as the 5′ UTR efficiently inhibited reporter gene expression to ≈1%. siRNAs also reduced the number of subgenomic replicon RNAs to ≈1%. In an alternative approach, pseudotyped retroviruses encoding shRNA were generated. A retroviral vector expressing shRNA targeting domain IV or nearby coding sequences inhibited reporter gene expression in Huh cells.

Takigawa et al. (215) utilized two methods to express shRNAs: one utilizing an expression plasmid and the other utilizing a recombinant lentivirus vector. The efficacy of a number of shRNAs directed against different target regions of the HCV genome in Huh cells transfected with HCV subgenomic replicon was determined. In both systems, shRNAs against NS3-1 (nucleotides 2052–2060) and NS5B (nucleotides 7326–7344) most efficiently suppressed expression of NS3 protein and reduced the amount of HCV replicon RNA.

The proteasome α-subunit PSMA7 modulates HCV-IRES activity in cell culture (216). The Hu antigen R (HuR) is a member of the ELAV-like protein family (217), which binds to HCV 3′ UTR RNA sequences (218).

Korf et al. (219) investigated the effect of a panel of DNA-based retroviral vectors expressing siRNAs against the highly conserved HCV-5′ and -3′ UTRs or the putative HCV cofactors PSMA7 and HuR on HCV IRES-mediated translation and subgenomic replication. siRNAs directed against highly conserved HCV-5′ and -3′ UTRs reduced HCV-IRES activity from the dual-gene luciferase reporter in Huh7 cells. These cells had been transfected with the dual-gene HCV-IRES reporter construct driven by the SV40 promoter to direct cap-dependent translation of renilla luciferase and cap-independent HCV IRES-mediated translation of FL. siRNAs inhibited HCV replicon RNA and HCV-NS5B protein expression in Huh cells harboring single-gene, subgenomic HCV replicons composed of regions such as the HCV 5′ UTR, nucleotides 342–389 of the core-encoding sequence, the HCV non-structural proteins NS3 to -5B, and the HCV 3′ UTR. siRNAs directed against PSMA7 and HuR reduced HCV-IRES activity from the dual-gene HCV-IRES reporter construct. siRNAs inhibited HCV replicon RNA and HCV-NS5B protein expression in Huh cells harboring single-gene, subgenomic HCV replicons. Selected combinations of HCV-directed siRNAs and siRNAs targeting PSMA7 and HuR or a combination of two siRNAs against these cofactors caused an additive inhibitory effect to that of subgenomic HCV replicons in Huh cells harboring single-gene, subgenomic HCV replicons.

HBV X protein induces HIV-1 replication and transcription through NF-κB binding sites in the HIV-1 long terminal repeat promoter (220). Specifically, the NS5a HCV protein activates NF-κB, in turn activating the promoter function of HIV-LTR (221,222).

Strayer et al. (223) exploited these findings to illustrate the potential applicability of such conditional expression approaches to drive the transcription of siRNA targeting HCV mRNA. siRNA was delivered with Tag-deleted SV40-derived vectors containing HIV-1 LTR. siRNA reduced the HCV-NS5A mRNA level by >98% in HepG2 cells stably expressing the HCV full genome. Specificity was confirmed by the finding that the siRNA delivered with the SV40-derived vector containing mutated HIV-1 LTR had no effect on the mRNA level.

Hamazaki et al. (224) synthesized shRNAs targeting the HCV IRES core gene transcript using T7 RNA polymerase and investigated the effect of shRNAs on the replication of HCV RNA in an HCV replicon stably expressing the HCV subgenome. shRNAs inhibited HCV replication by >90%. shRNAs did not induce luciferase activity in Huh7 cells or an HCV replicon transfected with a luciferase reporter gene-expressing vector with IFN-regulatory factor-3 binding regions. shRNAs did not induce IFN-β and did not activate PKR or 2′,5′-OAS in Huh7 cells and HCV replicon. These findings indicate that the shRNAs inhibit replication of HCV RNA without inducing an IFN response.

Inhibition of HBV gene expression and replication by RNAi

HBV is an enveloped virus with a partially ds relaxed-circular 3.2-kb DNA genome encoding polymerase, X protein, core antigen (C), and surface (PreS and S) (Fig. 2). With an estimated 400 million chronic carriers worldwide, HBV infection remains one of the most prevalent chronic viral infections in humans (225). Chronic infections have serious consequences, including cirrhosis and HCC (226), and are responsible for >1 million deaths annually (225). Current treatments for chronic HBV are suboptimal. Nucleoside or nt analogs, such as lamivudine and adefovir dipivoxil, suppress HBV replication effectively (227,228), but suffer from the selection of drug-resistant mutations and a high rate of relapse when treatment is discontinued (229). Although IFN-α and pegylated IFN-α have both immunomodulatory and antiviral effects, they achieve a sustained response in only a small percentage of patients and are usually associated with a wide array of side-effects (230,231). Thus, alternative therapeutic approaches for chronic HBV are needed. A number of groups have attempted to verify the usefulness of RNAi as a therapeutic tool in several model systems, as described below. The findings indicate that siRNA and shRNA against HBV efficiently interfere with HBV gene expression and replication.

McCaffrey et al. (232) investigated the effect of U6 shRNAs targeting C and S regions on the production of HBV intermediates in Huh7 cells, plus immunocompetent and immunodeficient mice transfected with a plasmid containing the HBV genome with some sequences duplicated to allow complete expression of all genes. shRNA reduced the amounts of HBsAg in culture medium and mouse serum by 94.2% and 84.5%, respectively. Immunohistochemistry indicated that shRNA reduced HBV core antigen (HBcAg) by >99%. Immunocompetent and immunocompromised mice treated with shRNA had 77% and 92% less HBV RNA, respectively. shRNA reduced HBV ss and ds DNA-replicative intermediates to undetectable levels.

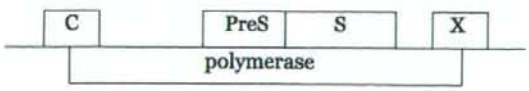

Fig. 2. Schematic representation of the HBV genome.

Giladi et al. (233) investigated the effect of siRNA targeting HBsAg on HBV gene expression and replication in both HepG2.2.215 cells transfected with HBV plasmid and in mice transfected with HBV plasmid. In their systems, injection of Balb/c mice with the HBV genomic plasmid resulted in the production and secretion of HBV-related antigens and replicative intermediates into the serum for >1 week. By 10 days, viral particle production subsides, concomitant with the appearance of anti-HBV antibodies. siRNA reduced the amount of HBsAg and HBV nucleocapsid antigen (HBeAg) in culture media by >80%. siRNA reduced HBV 3.6-kb and 2.1/2.4-kb mRNA species, and also reduced the amounts of HBsAg and HBeAg in mouse serum by 90% and 80%, respectively. Immunohistochemistry indicated that the siRNA diminished HBsAg-positive cells by >0.1%. siRNA reduced the three species of mRNAs by ≈50%. siRNA diminished HBV DNA in serum by >100-fold.

Konishi et al. (234) investigated the effect of siRNA targeting to polyadenylation (PA), precore (Prec), and S regions on replication of HBV in HepG2.2.215 cells transfected with HBV plasmid. HBsAg secretion into culture media was inhibited by 78%, 67%, and 42% with siRNAs against the PA, PreC, and S regions, respectively. siRNA against the PA region decreased levels of HBV pre-genomic RNA and HBV RNA containing the PA signal sequence by 72% and 86%, respectively. siRNA decreased the level of HBV core-associated DNA, a replication intermediate, by 71%. Immunohistochemistry indicated that siRNA decreased HBsAg-positive cells by 30–40%.

Shlomai and Shaul (235) investigated the effect of siRNA-producing vectors targeting the C and X ORF regions at the level of HBV proteins, transcripts, and HBV replicative forms in Huh and HepG2.2.15 cells. siRNAs against X and C regions significantly decreased levels of X and C proteins in Huh7 cells transfected with X and C region plasmids, respectively. siRNA against the X region significantly decreased the number of green fluorescent protein-positive cells in Huh7 cells transfected with HBV-GFP plasmid, in which the C

region was replaced with GFP. siRNA against the X region decreased core protein in HepG2.2.15 cells stably expressing HBV. siRNA against the X region decreased levels of all viral transcripts and viral replicative intermediates by ≈68% and ≈95%, respectively in Huh7 cells transfected with 1.3 X HBV genome plasmid. siRNA against the C region decreased levels of all viral transcripts and viral replicative intermediates by ≈13% and 40%, respectively in the Huh7 cells transfected with 1.3 X HBV genome plasmid.

Hamasaki et al. (236) investigated the effect of shRNA targeting to the core region on replication of HBV in Huh7 and HepG2 cells transfected with HBV genome plasmid. shRNA decreased the amount of HBeAg in culture media by 4.6- and 4.9-fold in Huh and HepG2 cells, respectively. shRNA decreased 3.5-kb mRNA of HBV plus the viral replicative intermediates, open circular and ss HBV-DNA in Huh cells.

Ying et al. (237) investigated the effect of siRNA targeting of the C region on viral replication in HepAD38 cells (producing wild-type virus) and HepAD59 cells (producing 3TC-resistant YMDD variant). siRNA inhibited viral DNA synthesis by 98% and 89% in HepAD38 cells and HepAD59 cells, respectively. siRNA decreased HBV core protein synthesis in HepAD38 cells, in which HBV replication was induced by removal of tetracycline from the culture medium.

Klein et al. (238) developed a novel mouse model to study HBV replication and investigated the effect of siRNA targeting of the ORFs of the S and C regions on expression of HBsAg and HBeAg using this model. In this model it is possible to introduce a replication-competent vector into hepatocytes and to activate HBV replication by a high-volume injection via the tail vein using an HBV replication-competent vector. siRNA targeting to the ORF of the S region decreased HBsAg and HBeAg in the serum by nearly 70% and 80%, respectively. siRNA decreased pre-C/C and S RNA levels in the liver. siRNA targeting to the ORF of the C region located outside the S region decreased HBeAg protein in serum and mRNA levels in the liver by 60% and 74%, respectively, whereas siRNA had no effect on the HBsAg protein level.

Chen et al. (239) investigated U6 shRNAs targeting different putative secondary structures on HBV pregenomic RNA, HBV RNA, and HBV replication in HepG2 cells transfected with HBV plasmids. Targeted sequences included direct repeat elements or regions coding for C, PreS, S, polymerase, and X protein. shRNAs decreased HBV RNA and the relative copy number of HBV DNA by up to 90% and by 90–97%, respectively.

Wu et al. (240) investigated the effect of plasmid-expressing siRNA targeting HBV C region nucleotides 2052–2070 on the replication and expression of HBV in mice transfected with HBV plasmid containing a 1.3-fold-overlength genome of HBV. siRNA decreased serum HBsAg and HBV C mRNA levels on Day 6 by ≈90% and 85%, respectively. Immunohistochemistry indicated that siRNA decreased HBcAg-positive cells from 5.4% to 0.9%.

Morrissey et al. (241) introduced some chemical modifications to siRNAs to improve their stability and investigated the effect of targeting siRNAs to the HBV genome in a mouse and a HepG2 cell model of HBV replication. The combination of modifications included 2′-fluoro, 2′-*O*-methyl, and 2′-deoxy sugars, phosphorothionate linkage, and terminus capping chemistries, plus complete removal of 2′-OH. The modified siRNA duplex prolonged the half-life ≈900-fold compared with the unmodified siRNA duplexes in 90% human serum at 37°C. The modified siRNA targeting a site located at starting 5′ nt 263 in the HBV genome decreased HBsAg in the culture media by ≈80% in HepG2 cells transfected with replication-competent HBV expression plasmid. The 263 siRNA decreased the HBV RNA level by 71% in mice transfected with complete HBV genome vector. The 263 siRNA and unmodified siRNA decreased serum HBV DNA by $10^{-3.7}$ and $10^{-2.2}$ at a dose of 1 μg. Similar results were obtained for serum HBsAg levels. When the 263 siRNA was delivered 3 days after transfection of the HBV vector it decreased serum HBV DNA levels by $10^{-0.9}$.

The same group (242) also synthesized stable nucleic acid–lipid particle (SNALP) formulations of stabilized siRNA, investigating its efficacy using several criteria. Stabilized siRNA-SNALP almost completely eliminated HBsAg protein in culture media of HepG2 cells transfected with HBV plasmid with an IC_{50} of ~1 nM. Stabilized siRNA-SNALP prolonged the half-life in plasma to approximately eightfold compared to stabilized siRNA in mice. Non-stabilized siRNA-SNALP strongly induced serum IFN-α or inflammatory cytokines (IL-6, TNF-α), plus serum aspartate aminotransferase and alanine aminotransferase, whereas such effects were not observed in the stabilized siRNA-SNALP. Stabilized siRNA-SNALP reduced serum HBV DNA by $>10^{-1.0}$ in a mouse model of HBV replication. The reduction in HBV DNA was dose-dependent and lasted for up to 6 weeks. Furthermore, reductions were seen in serum HBV DNA for up to 6 weeks with weekly dosing.

Uprichard et al. (243) investigated the effect of Ad vector expressing U6 RNA polymerase III-driven

shRNAs targeting HBV regions overlapping 3.5-, 2.4-, and 2.1-kb RNA on preexisting HBV gene expression and replication in HBV transgenic mice. The HBV-specific siRNA numbers, HBV 546 and HBV 765, refer to the initial nt of siRNA relative to the unique viral EcoRI site. shRNAs decreased the amount of HBsAg and HBeAg in serum by five- to sixfold on Day 4. The reduction in HBsAg and HBeAg levels continued until 13 days. shRNAs decreased the 2.1-kb envelope and 3.5-kb viral RNA in the liver by >50-fold and by four- to fivefold on Day 20, respectively. The same authors also did similar experiments using HBV transgenic mice that are genetically deficient for the expression of IFN-γ and the IFN-α/β receptor, as in vivo Ad does induce IFNs that clear HBV DNA from the liver. HBV 765 decreased HBsAg and HBeAg on Day 26 by ≈20-fold and 10-fold, respectively. HBV 765 decreased 2.1- and 3.5-kb RNA on Days 17–26 to an undetectable level and by 10-fold, respectively. This pattern of HBV RNA inhibition was maintained through to Day 26. HBV 765 decreased HBV replicative intermediate to virtually undetectable levels on Days 17–26. Immunohistochemistry indicated that HBV 765 decreased HBcAg-positive cells in the liver to an undetectable level on Days 17 and 26.

Wu et al. (244) investigated the effect of the human H1 promoter-encoded shRNAs targeting the S regions on the viral proteins, RNA, and DNA for three HBV genotypes in several models. shRNA decreased HBsAg and HBeAg protein in the culture media on Days 6 and 2 by 98.2% and 62.6%, respectively in Huh7 cells transfected with HBV genotype A plasmid. shRNA markedly decreased HBV RNA in cells and HBV replicative DNA in culture media and the cytoplasm. shRNA decreased HBsAg in the serum by >99% on Day 4 in mice transfected with HBV genotype A plasmid. Immunohistochemistry indicated that shRNA decreased HBcAg-positive cells in the liver by >95%. shRNA also decreased HBsAg and HBeAg in the culture media by ≈95% and 85%, respectively in Huh7 cells transfected with HBV genotype B or C plasmids. In these experiments, a clone from a patient with genotype C was resistant to shRNA. This mutant clone was found to exhibit a silent mutation in the target regions and could be selected out in the presence of shRNA in cell culture.

Carmona et al. (245) investigated the effect of a panel of shRNAs targeting the HBx ORF region on HBV replication in several models. To facilitate intracellular processing, the shRNAs included mismatches in the 25-bp stem region and a terminal loop of micro RNA-23. Two shRNAs (−5 and −6) decreased HBsAg secretion and HBV–GFP fusion marker protein without inducing IFN responses by >95% and ≈60% in Huh7 cells transfected with HBV plasmid and HBV–GFP fusion plasmid, respectively. The two shRNAs did not affect IFN response: induction of IFN-β, OAS1, and MxA in Huh7 cells. shRNAs decreased HBV RNA to ≈35% in Huh7 cells transfected with HBV plasmid. shRNA5 decreased HBsAg in serum to a background level over a period of 4 days in HBV transgenic mice. Immunohistochemistry indicated that shRNA5 decreased HBcAg-positive cells in the liver to an almost undetectable level. The two shRNAs decreased HBsAg and viral particle concentration in serum by >99% on Day 4 in mice. Carmona et al. incorporated the two shRNAs into an Ad vector to assess the antiviral efficacy of these shRNAs in a context similar to that of natural HBV infection. The two Ad vector shRNAs decreased HBsAg and HBeAg in serum by >90% and ≈50% by Day 12. Ad shRNAs −5 and −6 decreased the virion count in serum by 60% and 98% in mice, respectively.

Kim et al. (246) investigated the effect of siRNA and U6 shRNAs targeting positions 1374–1392 of the HBx sequence on the HBx mRNA level in HepG2-HBX expressing HBx mRNA and HepG2-K8 producing HBV particle. siRNA and tU6 shRNA reduced the HBx mRNA level by up to 80–90% in these cells. They also investigated the effect of siRNA and U6 shRNA on GFP expression in HepG2 cells transfected with HBx–eGFP fusion plasmid. siRNA and U6 shRNA reduced GFP expression by 90%. Chromosomal integration of U6 shRNA into HepG2 cells was also confirmed.

Chen et al. (247) investigated the effect of a ds adeno-associated virus eight-pseudotyped vector expressing shRNA targeting the S1 region of HBV on levels of HBV protein, mRNA, and replicative DNA in HBV transgenic mice. This shRNA decreased HBsAg protein and HBV genome in serum by >99% at 14 days. shRNA decreased 2.4/2.1- and 3.5-kb HBV transcripts by 93% and 81%, respectively. shRNA almost completely eliminated HBV replicative intermediates, intrahepatic relaxed-circular, and ss linear viral DNA. Immunohistochemistry indicated that shRNA almost completely eliminated HBcAg-positive cells in the liver. These reductions persisted for >120 days. Reductions in HBsAg, HBV DNA, and HBV replicative intermediates at 120 days were 66.1%, 77.1%, and 75.8%, respectively. shRNA induced only negligible amounts of IFN-γ and -β, and 2′,5′-OAS.

Acknowledgements

This work was supported by a Grant-in-Aid for Cancer Research (No. 15-2) from the Ministry of Health, Labor and Welfare of Japan.

References

1. Hannon GJ. RNA interference. Nature 2002;418:244–51.
2. McManus MT, Petersen CP, Haines BB, Chen J, Sharp PA. Gene silencing using micro-RNA designed hairpins. RNA 2002;8:842–50.
3. Hammond SM, Caudy AA, Hannon GJ. Post-transcriptional gene silencing by double-stranded RNA. Nat Rev Genet 2001;2:110–9.
4. Zamore PD. RNA interference: listening to the sound of silence. Nat Struct Biol 2001;8:746–50.
5. Hamilton AJ, Baulcombe DC. A species of small antisense RNA in posttranscriptional gene silencing in plants. Science 1999;286:950–2.
6. Hammond SM, Bernstein E, Beach D, Hannon GJ. An RNA-directed nuclease mediates post-transcriptional gene silencing in Drosophila cells. Nature 2000;404:293–6.
7. Zamore PD, Tuschl T, Sharp PA, Bartel DP. RNAi: double-stranded RNA directs the ATP-dependent cleavage of mRNA at 21 to 23 nucleotide intervals. Cell 2000;101:25–33.
8. Elbashir SM, Lendeckel W, Tuschl T. RNA interference is mediated by 21- and 22-nucleotide RNAs. Genes Dev 2001; 15:188–200.
9. Bernstein E, Caudy AA, Hammond SM, Hannon GJ. Role for a bidentate ribonuclease in the initiation step of RNA interference. Nature 2001;409:363–6.
10. Yang D, Lu H, Erickson JW. Evidence that processed small dsRNAs may mediate sequence-specific mRNA degradation during RNAi in Drosophila embryos. Curr Biol 2000;10: 1191–200.
11. Elbashir SM, Harborth J, Lendeckel W, Yalcin A, Weber K, Tuschl T. Duplexes of 21-nucleotide RNAs mediate RNA interference in cultured mammalian cells. Nature 2001;411: 494–8.
12. Stark GR, Kerr IM, Williams BR, Silverman RH, Schreiber RD. How cells respond to interferons. Annu Rev Biochem 1998;67:227–64.
13. Samuel CE. Antiviral actions of interferons. Clin Microbiol Rev 2001;14:778–809.
14. Yu JY, DeRuiter SL, Turner DL. RNA interference by expression of short-interfering RNAs and hairpin RNAs in mammalian cells. Proc Natl Acad Sci U S A 2002;99:6047–52.
15. Sui G, Soohoo C, Affar el B, Gay F, Shi Y, Forrester WC, et al. A DNA vector-based RNAi technology to suppress gene expression in mammalian cells. Proc Natl Acad Sci U S A 2002;99:5515–20.
16. Miyagishi M, Taira K. U6 promoter-driven siRNAs with four uridine 3′ overhangs efficiently suppress targeted gene expression in mammalian cells. Nat Biotechnol 2002;20: 497–500.
17. Paul CP, Good PD, Winer I, Engelke DR. Effective expression of small interfering RNA in human cells. Nat Biotechnol 2002;20:505–8.
18. Maeda I, Kohara Y, Yamamoto M, Sugimoto A. Large-scale analysis of gene function in Caenorhabditis elegans by high-throughput RNAi. Curr Biol 2001;11:171–6.
19. Waterhouse PM, Helliwell CA. Exploring plant genomes by RNA-induced gene silencing. Nat Rev Genet 2003;4:29–38.
20. Harborth J, Elbashir SM, Bechert K, Tuschl T, Weber K. Identification of essential genes in cultured mammalian cells using small interfering RNAs. J Cell Sci 2001;114: 4557–65.
21. Cottrell TR, Doering TL. Silence of the strands: RNA interference in eukaryotic pathogens. Trends Microbiol 2003;11:37–43.
22. Gitlin L, Andino R. Nucleic acid-based immune system: the antiviral potential of mammalian RNA silencing. J Virol 2003;77:7159–65.
23. Caplen NJ. RNAi as a gene therapy approach. Expert Opin Biol Ther 2003;3:575–86.
24. Li K, Lin SY, Brunicardi FC, Seu P. Use of RNA interference to target cyclin E-overexpressing hepatocellular carcinoma. Cancer Res 2003;63:3593–7.
25. Mitaka T, Sattler CA, Sattler GL, Sargent LM, Pitot HC. Multiple cell cycles occur in rat hepatocytes cultured in the presence of nicotinamide and epidermal growth factor. Hepatology 1991;13:21–30.
26. Mitaka T, Mikami M, Sattler GL, Pitot HC, Mochizuki Y. Small cell colonies appear in the primary culture of adult rat hepatocytes in the presence of nicotinamide and epidermal growth factor. Hepatology 1992;16:440–7.
27. Tateno C, Yoshizato K. Long-term cultivation of adult rat hepatocytes that undergo multiple cell divisions and express normal parenchymal phenotypes. Am J Pathol 1996;148: 383–92.
28. Tateno C, Yoshizato K. Growth and differentiation in culture of clonogenic hepatocytes that express both phenotypes of hepatocytes and biliary epithelial cells. Am J Pathol 1996;149:1593–605.
29. Niimi S, Oshizawa T, Yamaguchi T, Harashima M, Seki T, Ariga T, et al. Specific expression of annexin III in rat-small-hepatocytes. Biochem Biophys Res Commun 2003;300: 770–4.
30. Niimi S, Harashima M, Gamou M, Hyuga M, Seki T, Ariga T, et al. Expression of annexin A3 in primary cultured parenchymal rat hepatocytes and inhibition of DNA synthesis by suppression of annexin A3 expression using RNA interference. Biol Pharm Bull 2005;28:424–8.
31. Saltiel AR, Kahn CR. Insulin signalling and the regulation of glucose and lipid metabolism. Nature 2001;414:799–806.
32. Postic C, Dentin R, Girard J. Role of the liver in the control of carbohydrate and lipid homeostasis. Diabetes Metab 2004;30:398–408.
33. Chakravarty K, Cassuto H, Reshef L, Hanson RW. Factors that control the tissue-specific transcription of the gene for phosphoenolpyruvate carboxykinase-C. Crit Rev Biochem Mol Biol 2005;40:129–54.
34. Lee YH, Koh SS, Zhang X, Cheng X, Stallcup MR. Synergy among nuclear receptor coactivators: selective requirement for protein methyltransferase and acetyltransferase activities. Mol Cell Biol 2002;22:3621–32.
35. Koh SS, Chen D, Lee YH, Stallcup MR. Synergistic enhancement of nuclear receptor function by p160 coactivators and two coactivators with protein methyltransferase activities. J Biol Chem 2001;276:1089–98.
36. Krones-Herzig A, Mesaros A, Metzger D, Ziegler A, Lemke U, Bruning JC, et al. Signal-dependent control of gluconeogenic key enzyme genes through coactivator-associated arginine methyltransferase 1. J Biol Chem 2006;281:3025–9.
37. Camacho IA, Nagarkatti M, Nagarkatti PS. 2,3,7,8-Tetrachlorodibenzo-p-dioxin (TCDD) induces Fas-dependent activation-induced cell death in superantigen-primed T cells. Arch Toxicol 2002;76:570–80.

38. Cantrell SM, Joy-Schlezinger J, Stegeman JJ, Tillitt DE, Hannink M. Correlation of 2,3,7,8-tetrachlorodibenzo-p-dioxin-induced apoptotic cell death in the embryonic vasculature with embryotoxicity. Toxicol Appl Pharmacol 1998;148:24–34.
39. Christensen JG, Gonzales AJ, Cattley RC, Goldsworthy TL. Regulation of apoptosis in mouse hepatocytes and alteration of apoptosis by nongenotoxic carcinogens. Cell Growth Differ 1998;9:815–25.
40. Kamath AB, Xu H, Nagarkatti PS, Nagarkatti M. Evidence for the induction of apoptosis in thymocytes by 2,3,7,8-tetrachlorodibenzo-p-dioxin in vivo. Toxicol Appl Pharmacol 1997;142:367–77.
41. Kamath AB, Camacho I, Nagarkatti PS, Nagarkatti M. Role of Fas-Fas ligand interactions in 2,3,7,8-tetrachlorodibenzo-p-dioxin (TCDD)-induced immunotoxicity: increased resistance of thymocytes from Fas-deficient (lpr) and Fas ligand-defective (gld) mice to TCDD-induced toxicity. Toxicol Appl Pharmacol 1999;160:141–55.
42. McConkey DJ, Hartzell P, Duddy SK, Hakansson H, Orrenius S. 2,3,7,8-Tetrachlorodibenzo-p-dioxin kills immature thymocytes by Ca2+-mediated endonuclease activation. Science 1988;242:256–9.
43. Rhile MJ, Nagarkatti M, Nagarkatti PS. Role of Fas apoptosis and MHC genes in 2,3,7,8-tetrachlorodibenzo-p-dioxin (TCDD)-induced immunotoxicity of T cells. Toxicology 1996;110:153–67.
44. Sakamoto MK, Mima S, Tanimura TA. Morphological study of liver lesions in Xenopus larvae exposed to 2,3,7,8-tetrachlorodibenzo-p-dioxin (TCDD) with special reference to apoptosis of hepatocytes. J Environ Pathol Toxicol Oncol 1995;14:69–82.
45. Okey AB, Riddick DS, Harper PA. Molecular biology of the aromatic hydrocarbon (dioxin) receptor. Trends Pharmacol Sci 1994;15:226–32.
46. Schmidt JV, Su GH, Reddy JK, Simon MC, Bradfield CA. Characterization of a murine Ahr null allele: involvement of the Ah receptor in hepatic growth and development. Proc Natl Acad Sci U S A 1996;93:6731–6.
47. Park KT, Mitchell KA, Huang G, Elferink CJ. The aryl hydrocarbon receptor predisposes hepatocytes to Fas-mediated apoptosis. Mol Pharmacol 2005;67:612–22.
48. Ziegelbauer J, Shan B, Yager D, Larabell C, Hoffmann B, Tjian R. Transcription factor MIZ-1 is regulated via microtubule association. Mol Cell 2001;8:339–49.
49. Ziegelbauer J, Wei J, Tjian R. Myc-interacting protein 1 target gene profile: a link to microtubules, extracellular signal-regulated kinase, and cell growth. Proc Natl Acad Sci U S A 2004;101:458–63.
50. Lu TT, Makishima M, Repa JJ, Schoonjans K, Kerr TA, Auwerx J, et al. Molecular basis for feedback regulation of bile acid synthesis by nuclear receptors. Mol Cell 2000;6:507–15.
51. Delerive P, Galardi CM, Bisi JE, Nicodeme E, Goodwin B. Identification of liver receptor homolog-1 as a novel regulator of apolipoprotein AI gene transcription. Mol Endocrinol 2004;18:2378–87.
52. Zanjani ED, Poster J, Burlington H, Mann LI, Wasserman LR. Liver as the primary site of erythropoietin formation in the fetus. J Lab Clin Med 1977;89:640–4.
53. Dame C, Fahnenstich H, Freitag P, Hofmann D, Abdul-Nour T, Bartmann P, et al. Erythropoietin mRNA expression in human fetal and neonatal tissue. Blood 1998;92:3218–25.
54. Weiss MJ, Orkin SH. GATA transcription factors: key regulators of hematopoiesis. Exp Hematol 1995;23:99–107.
55. Aird WC, Parvin JD, Sharp PA, Rosenberg RD. The interaction of GATA-binding proteins and basal transcription factors with GATA box-containing core promoters. A model of tissue-specific gene expression. J Biol Chem 1994;269:883–9.
56. Nemer G, Nemer M. Transcriptional activation of BMP-4 and regulation of mammalian organogenesis by GATA-4 and -6. Dev Biol 2003;254:131–48.
57. Cirillo LA, Lin FR, Cuesta I, Friedman D, Jarnik M, Zaret KS. Opening of compacted chromatin by early developmental transcription factors HNF3 (FoxA) and GATA-4. Mol Cell 2002;9:279–89.
58. Goldberg MA, Glass GA, Cunningham JM, Bunn HF. The regulated expression of erythropoietin by two human hepatoma cell lines. Proc Natl Acad Sci U S A 1987;84:7972–6.
59. Dame C, Sola MC, Lim KC, Leach KM, Fandrey J, Ma Y, et al. Hepatic erythropoietin gene regulation by GATA-4. J Biol Chem 2004;279:2955–61.
60. Guo S, Rena G, Cichy S, He X, Cohen P, Unterman T. Phosphorylation of serine 256 by protein kinase B disrupts transactivation by FKHR and mediates effects of insulin on insulin-like growth factor-binding protein-1 promoter activity through a conserved insulin response sequence. J Biol Chem 1999;274:17184–92.
61. Puigserver P, Rhee J, Donovan J, Walkey CJ, Yoon JC, Oriente F, et al. Insulin-regulated hepatic gluconeogenesis through FOXO1-PGC-1alpha interaction. Nature 2003;423:550–5.
62. Schmoll D, Walker KS, Alessi DR, Grempler R, Burchell A, Guo S, et al. Regulation of glucose-6-phosphatase gene expression by protein kinase Balpha and the forkhead transcription factor FKHR. Evidence for insulin response unit-dependent and -independent effects of insulin on promoter activity. J Biol Chem 2000;275:36324–33.
63. Vander Kooi BT, Streeper RS, Svitek CA, Oeser JK, Powell DR, O'Brien RM. The three insulin response sequences in the glucose-6-phosphatase catalytic subunit gene promoter are functionally distinct. J Biol Chem 2003;278:11782–93.
64. Yeagley D, Guo S, Unterman T, Quinn PG. Gene- and activation-specific mechanisms for insulin inhibition of basal and glucocorticoid-induced insulin-like growth factor binding protein-1 and phosphoenolpyruvate carboxykinase transcription. Roles of forkhead and insulin response sequences. J Biol Chem 2001;276:33705–10.
65. Nakae J, Park BC, Accili D. Insulin stimulates phosphorylation of the forkhead transcription factor FKHR on serine 253 through a Wortmannin-sensitive pathway. J Biol Chem 1999;274:15982–5.
66. Rena G, Guo S, Cichy SC, Unterman TG, Cohen P. Phosphorylation of the transcription factor forkhead family member FKHR by protein kinase B. J Biol Chem 1999;274:17179–83.
67. Biggs WH 3rd, Meisenhelder J, Hunter T, Cavenee WK, Arden KC. Protein kinase B/Akt-mediated phosphorylation promotes nuclear exclusion of the winged helix transcription factor FKHR1. Proc Natl Acad Sci U S A 1999;96:7421–6.
68. Matsuzaki H, Daitoku H, Hatta M, Tanaka K, Fukamizu A. Insulin-induced phosphorylation of FKHR (Foxo1) targets to proteasomal degradation. Proc Natl Acad Sci U S A 2003;100:11285–90.
69. Rena G, Prescott AR, Guo S, Cohen P, Unterman TG. Roles of the forkhead in rhabdomyosarcoma (FKHR) phosphorylation sites in regulating 14-3-3 binding, transactivation and nuclear targetting. Biochem J 2001;354:605–12.
70. Zhang X, Gan L, Pan H, Guo S, He X, Olson ST, et al. Phosphorylation of serine 256 suppresses transactivation by

FKHR (FOXO1) by multiple mechanisms. Direct and indirect effects on nuclear/cytoplasmic shuttling and DNA binding. J Biol Chem 2002;277:45276–84.
71. Sotaniemi EA, Pelkonen O, Arranto AJ, Tapanainen P, Rautio A, Pasanen M. Diabetes and elimination of antipyrine in man: an analysis of 298 patients classified by type of diabetes, age, sex, duration of disease and liver involvement. Pharmacol Toxicol 2002;90:155–60.
72. Thummel KE, Schenkman JB. Effects of testosterone and growth hormone treatment on hepatic microsomal P450 expression in the diabetic rat. Mol Pharmacol 1990; 37:119–29.
73. Yamazoe Y, Murayama N, Shimada M, Yamauchi K, Kato R. Cytochrome P450 in livers of diabetic rats: regulation by growth hormone and insulin. Arch Biochem Biophys 1989; 268:567–75.
74. Kawamura A, Yoshida Y, Kimura N, Oda H, Kakinuma A. Phosphorylation/Dephosphorylation steps are crucial for the induction of CYP2B1 and CYP2B2 gene expression by phenobarbital. Biochem Biophys Res Commun 1999;264: 530–6.
75. Sidhu JS, Omiecinski CJ. Insulin-mediated modulation of cytochrome P450 gene induction profiles in primary rat hepatocyte cultures. J Biochem Mol Toxicol 1999;13:1–9.
76. Yoshida Y, Kimura N, Oda H, Kakinuma A. Insulin suppresses the induction of CYP2B1 and CYP2B2 gene expression by phenobarbital in adult rat cultured hepatocytes. Biochem Biophys Res Commun 1996;229:182–8.
77. Honkakoski P, Zelko I, Sueyoshi T, Negishi M. The nuclear orphan receptor CAR-retinoid X receptor heterodimer activates the phenobarbital-responsive enhancer module of the CYP2B gene. Mol Cell Biol 1998;18:5652–8.
78. Wei P, Zhang J, Egan-Hafley M, Liang S, Moore DD. The nuclear receptor CAR mediates specific xenobiotic induction of drug metabolism. Nature 2000;407:920–3.
79. Ueda A, Hamadeh HK, Webb HK, Yamamoto Y, Sueyoshi T, Afshari CA, et al. Diverse roles of the nuclear orphan receptor CAR in regulating hepatic genes in response to phenobarbital. Mol Pharmacol 2002;61:1–6.
80. Kodama S, Koike C, Negishi M, Yamamoto Y. Nuclear receptors CAR and PXR cross talk with FOXO1 to regulate genes that encode drug-metabolizing and gluconeogenic enzymes. Mol Cell Biol 2004;24:7931–40.
81. Brown MS, Goldstein JL. A receptor-mediated pathway for cholesterol homeostasis. Science 1986;232:34–47.
82. Eden ER, Patel DD, Sun XM, Burden JJ, Themis M, Edwards M, et al. Restoration of LDL receptor function in cells from patients with autosomal recessive hypercholesterolemia by retroviral expression of ARH1. J Clin Invest 2002; 110:1695–702.
83. Norman D, Sun XM, Bourbon M, Knight BL, Naoumova RP, Soutar AK. Characterization of a novel cellular defect in patients with phenotypic homozygous familial hypercholesterolemia. J Clin Invest 1999;104:619–28.
84. Wilund KR, Yi M, Campagna F, Arca M, Zuliani G, Fellin R, et al. Molecular mechanisms of autosomal recessive hypercholesterolemia. Hum Mol Genet 2002;11:3019–30.
85. Sirinian MI, Belleudi F, Campagna F, Ceridono M, Garofalo T, Quagliarini F, et al. Adaptor protein ARH is recruited to the plasma membrane by low density lipoprotein (LDL) binding and modulates endocytosis of the LDL/LDL receptor complex in hepatocytes. J Biol Chem 2005;280: 38416–23.
86. Schafer DF, Sorrell MF. Hepatocellular carcinoma. Lancet 1999;353:1253–7.
87. Geller SA. Hepatitis B and hepatitis C. Clin Liver Dis 2002; 6:317–34.
88. Iino S. Natural history of hepatitis B and C virus infections. Oncology 2002;62:18–23.
89. Nakamoto Y, Guidotti LG, Kuhlen CV, Fowler P, Chisari FV. Immune pathogenesis of hepatocellular carcinoma. J Exp Med 1998;188:341–50.
90. Fujii C, Nakamoto Y, Lu P, Tsuneyama K, Popivanova BK, Kaneko S, et al. Aberrant expression of serine/threonine kinase Pim-3 in hepatocellular carcinoma development and its role in the proliferation of human hepatoma cell lines. Int J Cancer 2005;114:209–18.
91. Deneen B, Welford SM, Ho T, Hernandez F, Kurland I, Denny CT. PIM3 proto-oncogene kinase is a common transcriptional target of divergent EWS/ETS oncoproteins. Mol Cell Biol 2003;23:3897–908.
92. Dyson N. The regulation of E2F by pRB-family proteins. Genes Dev 1998;12:2245–62.
93. Phillips AC, Vousden KH. E2F-1 induced apoptosis. Apoptosis 2001;6:173–82.
94. Sola S, Ma X, Castro RE, Kren BT, Steer CJ, Rodrigues CM. Ursodeoxycholic acid modulates E2F-1 and p53 expression through a caspase-independent mechanism in transforming growth factor beta1-induced apoptosis of rat hepatocytes. J Biol Chem 2003;278:48831–8.
95. Fan G, Ma X, Kren BT, Steer CJ. Unbound E2F modulates TGF-beta1-induced apoptosis in HuH-7 cells. J Cell Sci 2002;115:3181–91.
96. Schwarz JK, Bassing CH, Kovesdi I, Datto MB, Blazing M, George S, et al. Expression of the E2F1 transcription factor overcomes type beta transforming growth factor-mediated growth suppression. Proc Natl Acad Sci U S A 1995;92: 483–7.
97. Botla R, Spivey JR, Aguilar H, Bronk SF, Gores GJ. Ursodeoxycholate (UDCA) inhibits the mitochondrial membrane permeability transition induced by glycochenodeoxycholate: a mechanism of UDCA cytoprotection. J Pharmacol Exp Ther 1995;272:930–8.
98. Rodrigues CM, Fan G, Ma X, Kren BT, Steer CJ. A novel role for ursodeoxycholic acid in inhibiting apoptosis by modulating mitochondrial membrane perturbation. J Clin Invest 1998;101:2790–9.
99. Rodrigues CM, Ma X, Linehan-Stieers C, Fan G, Kren BT, Steer CJ. Ursodeoxycholic acid prevents cytochrome c release in apoptosis by inhibiting mitochondrial membrane depolarization and channel formation. Cell Death Differ 1999;6:842–54.
100. Rodrigues CM, Sola S, Sharpe JC, Moura JJ, Steer CJ. Tauroursodeoxycholic acid prevents Bax-induced membrane perturbation and cytochrome C release in isolated mitochondria. Biochemistry 2003;42:3070–80.
101. Tanaka H, Makino Y, Miura T, Hirano F, Okamoto K, Komura K, et al. Ligand-independent activation of the glucocorticoid receptor by ursodeoxycholic acid. Repression of IFN-gamma-induced MHC class II gene expression via a glucocorticoid receptor-dependent pathway. J Immunol 1996;156:1601–8.
102. Miura T, Ouchida R, Yoshikawa N, Okamoto K, Makino Y, Nakamura T, et al. Functional modulation of the glucocorticoid receptor and suppression of NF-kappaB-dependent transcription by ursodeoxycholic acid. J Biol Chem 2001; 276:47371–8.
103. Bailly-Maitre B, de Sousa G, Boulukos K, Gugenheim J, Rahmani R. Dexamethasone inhibits spontaneous apoptosis in primary cultures of human and rat hepatocytes via Bcl-2 and Bcl-xL induction. Cell Death Differ 2001;8:279–88.
104. Yamamoto M, Fukuda K, Miura N, Suzuki R, Kido T, Komatsu Y. Inhibition by dexamethasone of transforming growth factor beta1-induced apoptosis in rat hepatoma cells: